Received: 24 January 2023 | Revised: 10 March 2023 | Accepted: 13 March 2023

DOI: 10.1002/ppap.202300010

SCIENTIFIC PERSPECTIVE

PLASMA PROCESSES AND POLYMERS

Plasma activation mechanisms governed by specific energy input: Potential and perspectives

Dirk Hegemann

Empa, Swiss Federal Laboratories for Materials Science and Technology, Plasma & Coating Group, St.Gallen, Switzerland

Correspondence
Dirk Hegemann, Empa, Swiss Federal Laboratories for Materials Science and Technology, Plasma & Coating Group, Lerchenfeldstrasse 5, 9014 St.Gallen, Switzerland.
Email: dirk.hegemann@empa.ch

Abstract

In a low-temperature plasma, the electrons pick up energy from the electric field in collisions with atoms and molecules, gaining high kinetic energy that must be sufficient for ionizing reactions to sustain the plasma. For molecular gases, an average energy per heavy gas particle is thus available in the plasma, the specific energy input, yielding plasma activation by inelastic collisions. Following a distribution law, the probability for the activation mechanism can be described by an Arrhenius-like equation. The potential of this approach is demonstrated on the basis of plasma polymerization and plasma CO_2 conversion. For perspective, energy efficiencies are discussed as a function of conversion indicating the optimum that can be achieved by electron impact activation compared with additional ways of energy transfer, probably depending on certain constraints.

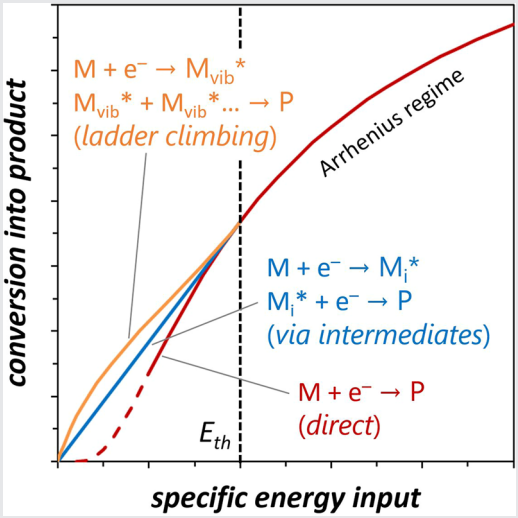

KEYWORDS

cold plasma, energy input, gas conversion, plasma chemistry, plasma polymerization

1 | INTRODUCTION

The specific energy input (SEI) describes the average energy available per molecule in a low-temperature plasma yielding plasma-chemical reactions such as excitation, dissociation, and ionization. This concept has already been developed in the 19th century regarding plasma synthesis of ozone as described by the "Becker formula" and has been further applied to various plasma gas conversion processes.[1,2] In 1969, Neiswender

Scientific Perspectives (expert opinion)

introduced the amount of energy absorbed per mole of monomer to qualitatively describe the conversion of benzene in a low-pressure plasma into a solid polymer.[3] In the late 1970ies, Yasuda further elaborated on this concept for plasma polymerization.[4] At low SEI, deposition rates of plasma polymer films typically increase linearly with energy input, approaching saturation at higher energies. From this general trend of deposition rates as a function of SEI, it was realized that the behavior above an apparent activation energy can be described by an Arrhenius-like equation with SEI replacing temperature.[5] Meanwhile, this approach was demonstrated to be applicable for many different monomers, that is, polymerizable molecules, yielding plasma polymerization.[6–11] Moreover, the concept also comprises the use of power modulation by applying on/off pulses to reduce the average power input in the plasma aiming to enhance the structural retention of monomers.[12,13] Likewise, replacing temperature by SEI following an Arrhenius-like form might be useful for plasma conversion, plasma catalysis, and plasma jet sintering[14–16]—though this is still a debated subject.[17] Therefore, this work aims in giving a more solid foundation for plasma activation mechanisms governed by the SEI, showing Arrhenius-like behavior (or deviations thereof).

Conventionally, chemical reactions are activated by temperature, which can be assisted by the presence of a catalyst. For two colliding molecules, for example in a gas (but not limited to it), a chemical reaction might occur depending on an activation barrier, E_a. At a given temperature, there is a distribution of kinetic energies for all the molecules (Boltzmann distribution). For reactants gaining kinetic energies above E_a (here, in [J]), provided by the temperature T, the probability for their reaction follows a distribution law, giving the rate resulting in a reaction

$$\varrho = A \exp\left(-\frac{E_a}{k_B T}\right), \tag{1}$$

with a pre-exponential factor, A, and Boltzmann constant, k_B.[18,19] The probability that colliding particles have sufficient energy to react is given by the exponential term of the equation, giving the portion of collisions with energies above E_a, while A gives the probability that particles with sufficient energy to react do react, which also involves orientation effects. For $k_B T = E_a$, thus not all collisions result in a reaction but only a fraction of $exp(-1) \approx 0.368$ at maximum. This phenomenological approach has been advanced by Svante Arrhenius in 1889 and holds for many molecules unless internal energy or steric factors become important.[20] The reaction rate, ϱ, depends on kinetic energy, the type of reaction partners and on other factors such as catalyst presence. It should be noted that for most chemical reactions, the validity of Equation (1) is limited to a restricted temperature range.[21] In some cases, the T-dependence of the pre-exponential factor, A', needs to be considered yielding the modified Arrhenius equation

$$\varrho = A'\, T^m \exp\left(-\frac{E_a}{k_B T}\right), \tag{2}$$

whereby its validity can be extended to a broader temperature range.[21,22] Note that the Arrhenius equation typically describes bimolecular chemical reactions with hard sphere interaction.

Similar to the above-described temperature-driven chemical reactions, energy provided by a weakly ionized plasma can also trigger chemical reactions (with a threshold energy) without the need for a heat source. Low-temperature (cold) plasmas are electrical gas discharges that gain their energy from the electric field in electron-neutral collisions without substantially heating the heavy gas particles. To sustain the plasma, electron energies reach the ionization potential of the used gas and thus also deliver sufficient kinetic energy for excitation and dissociation of any atom/molecule in the plasma. When sufficient electron–electron scattering takes place, the energy distribution of electrons can be described by a Maxwellian distribution function, which maximizes the entropy of the system.[23] Note that despite a low ionization degree (typically 10^{-4} to 10^{-6}), the total electron–electron scattering cross section is rather large, that is, $\sigma_{e-e} \approx 3{\cdot}10^{-12}$ cm^2 for an electron temperature, T_e, around 1 eV.[24] Electron-neutral collisions have three to four orders of magnitude lower cross sections (up to about 10^{-15} cm^2) as shown for Ar and CO_2 in Figure 1.[25,26] Furthermore, only the high-energy electrons of the electron energy distribution function (EEDF) cause inelastic scattering in noble gases by energy transfer exceeding the threshold energies. Hence, inelastic collisions result in a depletion of high-energy electrons affecting the EEDF, however, a "nearly" Maxwellian EEDF might be maintained.[27] Molecular gases such as CO_2, on the contrary, have much lower threshold energies for (vibrational) excitation and the total cross section is comparable to the cross section of elastic collisions.

A Maxwellian EEDF has been added in Figure 1, showing the distribution of the electron impact energy, ϵ, for a given T_e (here, in [eV])

$$f(\epsilon) = \frac{2\pi}{(\pi T_e)^{3/2}} \sqrt{\epsilon} \exp\left(-\frac{\epsilon}{T_e}\right), \tag{3}$$

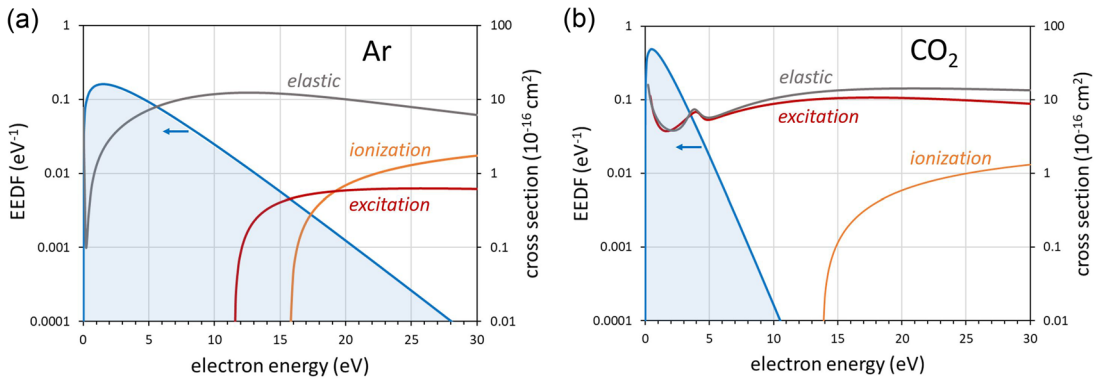

FIGURE 1 (a) Electron energy distribution function (EEDF) for $T_e = 3$ eV and electron impact cross sections of Ar for elastic and inelastic scattering. Excitation has a threshold energy of ~11.5 eV and ionization of 15.76 eV. (b) EEDF for $T_e = 1$ eV and electron impact cross sections of CO_2 for elastic and inelastic scattering. Excitation already starts at low energy, while ionization has a threshold of 13.8 eV. Analytical approximations for cross sections of Ar and CO_2 are taken from the literature.[25,26]

noting that the mean electron energy taken up by the electrons from the electric field is

$$\bar{\varepsilon} = \frac{3}{2}T_e = \frac{1}{2}m_e\bar{v}_e^2, \tag{4}$$

with the electron mass, m_e, and electron thermal velocity, $\bar{v}_e$. T_e is largely independent of discharge power or plasma density, which is applicable for all kinds of low-pressure discharges, that is, direct current (DC) or high frequency (HF) with radio frequency (RF) or microwave (MW) excitation.[27] Considering an EEDF at a typical T_e (e.g., 3 eV in Ar plasma), most electron-neutral collisions in a noble gas plasma are elastic, that is, low momentum transfer collisions (gas heating). However, with increasing electric field (or $T_e > 1$ eV), the electron energy loss is deposited mainly into the inelastic channels, that is, energy is transferred.[28,29] On the contrary, energy transfer already starts at much lower threshold energies for molecular gases due to the many ways for excitation, which is crucial for the discussion of plasma activation mechanism.

2 | PLASMA ACTIVATION MECHANISMS

In this section, the plasma activation in ionizing collisions and, in more general, in inelastic collisions is discussed providing the fundamentals to introduce the SEI.

2.1 | Arrhenius-like behavior of ionizing collisions in a plasma

Applying an electric field between electrodes in a gas, electrons with an initial density of n_0 are accelerated in z-direction by the uniform electric field, E_p, that is, inducing a drift velocity following the field vertical to the electrode. According to the classical Townsend mechanism, electrical breakdown occurs in the gas, when the kinetic energy of an electron exceeds the threshold for ionization, allowing neutral gas atoms or molecules to be ionized by electron impact.[30] To ignite (and sustain) a plasma, multiplication of charges in the gas is caused by further collisions of electrons with the heavy gas particles under the action of the electric field.[31] The ionization probability that the mean free path length of electrons for ionizing collisions, $\lambda_{\mathrm{ion},\|}$, parallel to the field (following a distribution law) exceeds the ionization length, z_{ion}, (in z-direction), which corresponds to the path length of electrons in the electric field to achieve the necessary translational energy for ionization, is then given by

$$P_{\mathrm{ion}} = \frac{n_e(z)}{n_0} = \exp\left(-\frac{z_{\mathrm{ion}}}{\lambda_{\mathrm{ion},\|}}\right), \tag{5}$$

which considers ionization as a chemical reaction.[24,31,32] Due to the distribution law (Boltzmann distribution) thus only the fraction $exp(-1)$ of all electrons traveling on average the length of $\lambda_{\mathrm{ion},\|} = z_{\mathrm{ion}}$ actually cause an ionizing collision. The electron energy gain in the field over z_{ion} is set equal to the ionization energy, E_{ion} (here, in [eV]) by

$$E_{\mathrm{ion}} = eE_p z_{\mathrm{ion}}. \tag{6}$$

The first Townsend coefficient, the probable number of ionizing collisions per length, dividing P_{ion} by $\lambda_{\mathrm{ion},\|}$, is expressed by[24,31,33,34]

$$\alpha_T = \frac{1}{\lambda_{\mathrm{ion},\|}}P_{\mathrm{ion}} = \frac{1}{\lambda_{\mathrm{ion},\|}}\exp\left(-\frac{E_{\mathrm{ion}}}{eE_p\,\lambda_{\mathrm{ion},\|}}\right). \tag{7}$$

The rate of ionization (per colliding electron per second) in the Townsend breakdown mechanism is then given by

$$\nu_{\text{ion}} = \alpha_T \, v_{e,\parallel} = \frac{v_{e,\parallel}}{\lambda_{\text{ion},\parallel}} \exp\left(-\frac{E_{\text{ion}}}{eE_p \, \lambda_{\text{ion},\parallel}}\right), \tag{8}$$

regarding the electron collisional drift velocity, $v_{e,\parallel}$.[35,36] Note that the translational motion parallel to the field is considered here (denoted by $\parallel$) yielding field-depending quantities. The collision frequency for ionization, ν_{ion}, on the contrary, which is the average of the related cross section over a Maxwellian distribution, is independent of plasma density and discharge power (and thus independent of the electric field).[27] Moreover, single-electron ionization with one type of gas is considered. Although the drift velocity is typically lower than the mean electron velocity, $\bar{v}_e$, of electrons moving in all directions, an electron can accumulate a tremendous amount of energy by drifting in the electric field, which is repeatedly reduced in inelastic collisions.[37] Hence, the fast electrons of the translational motion originating from the (thermal) mean electron velocity are responsible for ionizing collisions in the classical Townsend mechanism, comprising a swarm of electrons having both a random and a drift velocity.[31] Note that the distinction between random and drift velocity is only for mathematical convenience and has no physical significance, the same holds for the mean free path lengths considered to be parallel to the field. However, only those electrons moving in field direction contributing to the drift velocity can draw energy from the field.

The pre-exponential factor in Equation (8) can be considered as the ultimate rate for electron impact ionization if all molecules were to get ionized, thus defined as

$$\nu_{\text{ion},0} = \frac{v_{e,\parallel}}{\lambda_{\text{ion},\parallel}}, \tag{9}$$

related to electron drift velocity and mean free path length in field direction, as illustrated in Figure 2. While $\nu_{\text{ion},0}$ might only be approached for very high electric fields, a sufficiently large field is required to ignite and sustain the discharge.

Following the discussion as given, for example, by von Engel,[35] the electron drift velocity in sufficiently large electric fields can be found by balancing the energy gained per electron per second, θ_{abs}, (in [eV s^{-1}]) against that lost by electron-neutral collisions at the rate ν_c, when $\delta\bar{\varepsilon}$ is the energy loss per collision with the mean

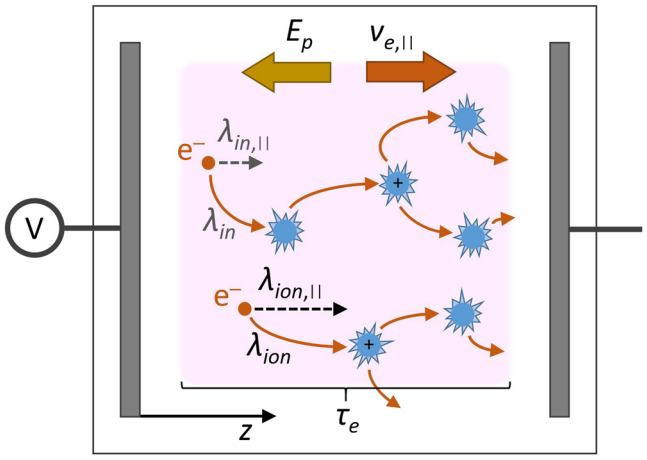

FIGURE 2 Drift velocity, $v_{e,\parallel}$, in *the* z-direction of an electron comprising the random (thermal) and superimposed drift motion by the electric field, E_p. While the electron gains energy in elastic collisions during the residence time, τ_e, in the plasma being accelerated in field direction, it transfers energy in inelastic collisions (excitation and ionization), changing direction and again starting acceleration on average in the field direction. The ideal (minimum) mean free path for ionizing collisions, $\lambda_{\text{ion},\parallel}$, or (in general) inelastic collisions, $\lambda_{in,\parallel}$, parallel to the field is indicated by dashed arrows.

electron impact energy, $\bar{\varepsilon}$, and the average fraction of energy lost, δ (energy transfer coefficient), yielding[29,38]

$$\theta_{\text{abs}} = eE_p v_{e,\parallel} = \delta\bar{\varepsilon}\,\nu_c. \tag{10}$$

The drift velocity of the electrons in the electric field can be related to the thermal velocity using the electron mobility parallel to the field[39]

$$\mu_e = \frac{v_{e,\parallel}}{E_p} = \frac{e}{m_e \nu_c}. \tag{11}$$

Using Equation (10), it follows that (in [eV m^{-1}])

$$eE_p = v_{e,\parallel} m_e \nu_c = \frac{\delta\bar{\varepsilon}\,\nu_c}{v_{e,\parallel}}. \tag{12}$$

With Equation (4), the ratio of drift velocity to thermal velocity of the electrons can eventually be given as

$$\frac{v_{e,\parallel}}{\bar{v}_e} = \sqrt{\frac{\delta}{2}}. \tag{13}$$

This ratio is solely dependent on the energy transfer coefficient within the validity of this approximation, since only the electrons moving in field direction draw energy from the field. Since δ increases with T_e,[29] $v_{e,\parallel}$

growths even stronger with T_e. Note that electrons have much higher velocities in the plasma than neutrals and still higher velocities compared with ions of comparable kinetic energy due to the low electron mass. Remarkably, with Equations (10) and (12), the absorbed power per electron per second becomes

$$\theta_{\text{abs}} = m_e v_{e,\parallel}{}^2 \nu_c, \tag{14}$$

thus depending on the "kinetic energy" of the electron drift motion in the plasma electric field.

For the purpose here, the classical Townsend description has thus been followed.[31] The first Townsend coefficient, the probable number of ionizing collisions per length in field direction, normalized to the gas number density, N, can then be expressed as

$$\alpha_T/N = \frac{\nu_{\text{ion},0}}{N\, v_{e,\parallel}} \exp\left(-\frac{E_{\text{ion}}}{eE_p \frac{v_{e,\parallel}}{\nu_{\text{ion},0}}}\right) = \frac{k_{\text{ion},0}}{v_{e,\parallel}} \exp\left(-\frac{E_{\text{ion}}}{eE_p/N \frac{v_{e,\parallel}}{k_{\text{ion},0}}}\right) = A \exp\left(-\frac{A\, E_{\text{ion}}}{eE_p/N}\right), \tag{15}$$

with the related ultimate rate coefficient for electron-neutral impact ionization, $k_{\text{ion},0}$, and the parameter, A, depending on the type of gas. Note that $k_{\text{ion},0}$ is a constant for a given gas. The ionization probability is thus governed by the reduced electric field, E_p/N. The first derivative of the exponential function of Equation (15) yields the Stoletow point (named after Alexander Stoletow), which provides the optimum $(E_p/N)_{\text{opt}}$ for ionization and the minimum of the Paschen breakdown curve for gases.[24,32] Based on measurements of α_T/N versus E_p/N for ionization in various (not contaminated) gases,[24,31,33,34] the range of validity of this simple Arrhenius-like expression was found to yield a good agreement for $(E_p/N)_{opt}/2 \le E_p/N \le 3(E_p/N)_{\text{opt}}$.[32] It should be noted, however, that A in Equation (15) is not a true constant, as often considered, but also depends on the electric field affecting the drift velocity.[24]

It has been argued that an effective ionization energy E^* might be taken instead of E_{ion} with $E^* = E_{\text{ion}}/a$, where $a < 1$, since an electron will lose energy by various collisions besides ionization.[32] Furthermore, it can be considered that, within certain limits, the energy which is transferred to the electron scales with E_p/N.[37] The ionization probability according to the Townsend mechanism can thus also be related to the distribution of the electron impact energy, ϵ, with its mean value, $\bar{\epsilon}$. Based on Equations (10) and (15), it follows that

$$P_{\text{ion}} = \exp\left(-\frac{E^*}{eE_p \frac{v_{e,\parallel}}{\nu_{\text{ion},0}}}\right) = \exp\left(-\frac{E_{\text{ion}}\, \nu_{\text{ion},0}}{a\, \theta_{\text{abs}}}\right) = \exp\left(-\frac{E_{\text{ion}}\, \nu_{\text{ion},0}}{a\, \delta\nu_c\, \epsilon}\right). \tag{16}$$

This approach also enables to unify DC and HF descriptions, since the loss mechanism (energy transfer) in the plasma is comparable.[29] Further discussion on electron motion in DC and HF plasmas can be found in the literature.[37,39] Regarding that the main loss channels for the absorbed power of electrons in the field are inelastic collisions (excitation, ionization, and potentially dissociation),[29,40] where only the fraction a (<1) is lost into ionizing collisions, it can be noted for the energy lost per ionizing collision per second that

$$\theta_{l,\text{ion}} = a\theta_{\text{abs}} = \nu_{\text{ion},0} \langle E \rangle = a\nu_{\text{in},0} \quad \langle E \rangle, \tag{17}$$

with an (averaged) plasma energy available for ionization, $<E>$, exceeding E_{ion}. Here, the ultimate collision frequency, $\nu_{\text{in},0}$, for the total inelastic scattering in the plasma is introduced. Hence, $a = \nu_{\text{ion},0}/\nu_{\text{in},0}$. With Equation (10), it follows that

$$\nu_{\text{ion},0} = \frac{\theta_{l,\text{ion}}\, \nu_{\text{in},0}}{\delta\epsilon\nu_c}. \tag{18}$$

With Equations (17) and (18), the ionization in the field per length and per particle density, the equivalent of an ionization cross-section, can eventually be expressed as

$$\alpha_T/N = \frac{\nu_{\text{ion},0}}{N\, v_{e,\parallel}} P_{\text{ion}} = \frac{\theta_{l,\text{ion}}}{N\, v_{e,\parallel}} \frac{\nu_{\text{in},0}}{\delta\nu_c}\, \epsilon^{-1} \exp\left(-\frac{\nu_{\text{in},0}}{\delta\nu_c} \frac{E_{\text{ion}}}{\epsilon}\right). \tag{19}$$

Figure 3 compares Equation (19) to ionization cross sections for various gases using analytical approximations as given in the literature.[25,26,41] Note that for $\epsilon \le E_{\text{ion}}$, the probability of a direct (one-step) electron impact ionization process to occur is zero. With increasing energy above E_{ion}, the probability is known to rise at first and after passing a maximum to decrease again.[31] For $\epsilon > E_{\text{ion}}$, a reasonable good agreement can be observed between the ionization cross section, σ_{ion}, and α_T/N, which considers ionization as a plasma-chemical reaction. Further modifications of this simplified Arrhenius-like equation (also including Coulomb interaction for electron-ion collisions) might be introduced,[42] which is outside the scope of this work.

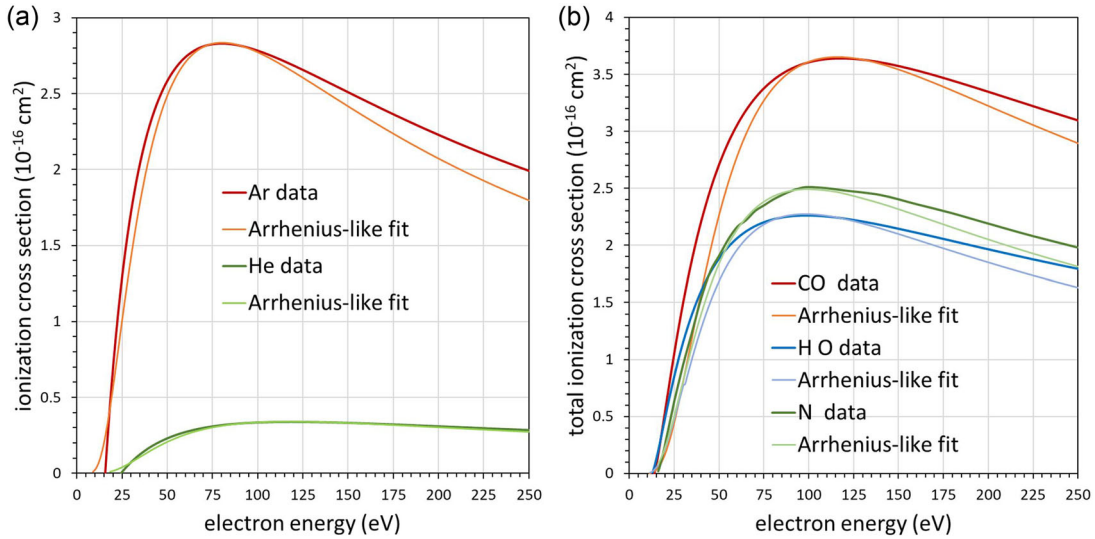

FIGURE 3 (a) Ionization of cross sections for inert gases and (b) total ionization across sections for molecular gases using analytical approximations of experimental data.[25,26,41] Fitting is based on the Arrhenius-like curve according to Equation (19), matching the optimum cross section.

The optimum cross section based on Equation (19) yields

$$\epsilon_{\text{opt}} = \frac{\nu_{\text{in},0}}{\delta \nu_c} E_{\text{ion}}. \tag{20}$$

and for the pre-exponential factor

$$A(\epsilon_{\text{opt}}) = \frac{\theta_{l,\text{ion}}}{N \nu_{e,\parallel} E_{\text{ion}}}. \tag{21}$$

The average power lost per electron into ionization, $\theta_{l,\ ion}/N$, normalized to the gas density, is dependent on T_e but also on $v_{e,\parallel}$ according to Equation (14).[29,35]

Table 1 lists the obtained values from the fitting for the considered gases. It can be seen that substantial ionization, for example, of 36.8% at ϵ_{opt}, requires high electron temperatures (about 50–80 eV) considering Equation (4), which is why the ionization degree in low-temperature plasmas is typically only around 10^{-6}–10^{-4}. The factor a (in the last column) denotes the fraction of energy transferred to ionizing collisions for energies exceeding E_{ion}, that is, at high ϵ, as taken from the literature.[32] For inert gases, most of the energy is thus transferred to ionization, whereas molecular gases still show a substantial contribution by other inelastic collisions at high electron energies. Note that other plasma reaction rates such as, for example, dissociative electron attachment to an ozone molecule might also follow a modified Arrhenius form as given by Equation (19).[43]

TABLE 1 Fitting parameters as used in Figure 3 for the Arrhenius-like approach to describe ionization cross sections in different gases depending on electron impact energies.

Gas	E_{ion} (eV)	ϵ_{opt} (eV)	$\epsilon_{\text{opt}}/E_{\text{ion}}$ (-)	$A(\epsilon_{\text{opt}})$ (10^{-16} cm^2)	$a = E_{\text{ion}}/E^*$ (from [32])
Ar	15.76	80.4	5.1	7.71	0.94
He	24.59	118	4.8	0.92	0.88
N_2	15.58	99.7	6.4	6.77	0.49
CO_2	13.8	116	8.4	9.92	0.60
H_2O	12.6	97.0	7.7	6.18	0.57

The field-independent ionization frequency is related to the first Townsend coefficient by

$$\nu_{\text{ion}} = N \langle \sigma_{\text{ion}} v_e \rangle = \int_0^\infty \sigma_{\text{ion}} (2\epsilon/m_e)^{1/2} f(\epsilon) d\epsilon = \alpha_T \tag{22}$$

$$\nu_{e,\parallel} = \nu_{\text{ion},0}\, P_{\text{ion}},$$

with $f(\epsilon)$ according to Equation (3) for Maxwellian electrons.[35] The right-hand side of Equation (22), however, is not only depending on ϵ (for a given T_e), but also on electron drift velocity. Hence, $\epsilon_{\text{opt}}/E_{\text{ion}}$ and $A(\epsilon_{\text{opt}})$ are not true constants. The random and drift motion of the swarm of electrons result in a different (physical) mean free path for ionization collisions, λ_{ion}, as compared with the ideal (mathematical) pathway, $\lambda_{\text{ion},||}$, in z-direction yielding ionization (see Figure 2). Note that electrons might undergo several inelastic

collisions with frequencies, $\nu_{\mathrm{ion},i}$, during the electron confinement time, τ_e, of one electron in the plasma, which can be estimated by

$$\tau_e = \frac{1}{\sum_i \nu_{\mathrm{ion},i}} = \frac{1}{\nu_{\mathrm{ion}}}, \tag{23}$$

assuming that T_e is constant.[40] The right-hand side holds for gases forming only one type of ion as considered so far. Equation (23) is thus a simplified condition to sustain the plasma (neglecting secondary electrons and ion losses).

Furthermore, a mixture of two gases (or generally two possibilities in the plasma to form ions) can be treated by using an additive model in which the ionization densities produced in the mixed gas is the sum of the densities in each gas

$$P_{\mathrm{ion}} = p_1 \exp\left(-\frac{E_{\mathrm{ion},1}(p_1\nu_{\mathrm{ion},\parallel,1} + p_2\nu_{\mathrm{ion},\parallel,2})}{aeE_p\nu_{e,\parallel}}\right) + p_2 \exp\left(-\frac{E_{\mathrm{ion},2}(p_1\nu_{\mathrm{ion},\parallel,1} + p_2\nu_{\mathrm{ion},\parallel,2})}{aeE_p\nu_{e,\parallel}}\right), \tag{24}$$

where p_1 and p_2 are the relative partial pressures, $E_{\mathrm{ion},1}$ and $E_{\mathrm{ion},2}$ the ionization energies and $\nu_{\mathrm{ion},\parallel,1}$ and $\nu_{\mathrm{ion},\parallel,2}$ the ionization frequencies of the two gases parallel to the electric field.[34] Regarding Equations (16) and (17), it can be noted that

$$aeE_p\nu_{e,\parallel} = a\theta_{\mathrm{abs}} = \theta_{l,\mathrm{ion}} = (p_1\nu_{\mathrm{ion},\parallel,1} + p_2\nu_{\mathrm{ion},\parallel,2})\langle E\rangle \tag{25}$$

provided that the available energy for ionization, $<E>$, exceeds the ionization energies. Hence, Arrhenius-like expressions can be added up using an averaged plasma energy[44]

$$P_{\mathrm{ion}} = p_1\exp\left(-\frac{E_{\mathrm{ion},1}}{\langle E\rangle}\right) + p_2\exp\left(-\frac{E_{\mathrm{ion},2}}{\langle E\rangle}\right). \tag{26}$$

2.2 | SEI

To overcome issues by relating the probability for chemical reactions in a plasma to either the (reduced) electric field, E_p/N (Equation (15)), or the electron impact energy, ϵ (Equation (19)), yielding "constants" that might actually be dependent on both parameters, as noticed above, the SEI can be introduced, which will be discussed in the following. Here, molecular gases are considered to allow multiple excitation and dissociation collisions already at low SEI.

In a more general framework, the probability, P_{in}, that an inelastic chemical (activation) reaction might take place in a molecular gas passing through a low-temperature plasma, can be derived analogous to the Townsend mechanism. The fraction of excited molecules, c_{in}, over the length z_{in} in the electric field yielding an inelastic collision with respect to the maximum conversion of the molecule, c_0 (for a given experimental set-up), can then be noted as

$$P_{\mathrm{in}} = \frac{c_{\mathrm{in}}(z)}{c_0} = \exp\left(-\frac{z_{\mathrm{in}}}{\lambda_{\mathrm{in},\parallel}}\right), \tag{27}$$

for the case that the mean free path length of electrons for the inelastic collision, $\lambda_{\mathrm{in},\parallel}$ (in z-direction), following a distribution law exceeds the length, z_{in}. As discussed above for ionization, the electron energy gain over z_{in} can be set equal to a threshold energy, an apparent activation energy, E_{th} (in [eV])

$$E_{\mathrm{th}} = eE_p z_{\mathrm{in}}, \tag{28}$$

yielding

$$P_{\mathrm{in}} = \frac{c_{\mathrm{in}}(z)}{c_0} = \exp\left(-\frac{E_{\mathrm{th}}}{eE_p\,\lambda_{\mathrm{in},\parallel}}\right). \tag{29}$$

Since the denominator in the exponential term is equivalent to an energy, the average energy available per molecule in the plasma, the SEI, can simply be defined as

$$E_{\mathrm{pl}} = eE_p\lambda_{\mathrm{in},\parallel}. \tag{30}$$

Following the Arrhenius-like formalism as for the Townsend mechanism as in Equation (8), the collision rate for inelastic collisions is then expressed by

$$\nu_{in} = \frac{\nu_{e,\parallel}}{\lambda_{\mathrm{in},\parallel}}\exp\left(-\frac{E_{\mathrm{th}}}{eE_p\,\lambda_{\mathrm{in},\parallel}}\right) = \nu_{\mathrm{in},0}\exp\left(-\frac{E_{\mathrm{th}}}{E_{\mathrm{pl}}}\right), \tag{31}$$

which holds for $E_{pl} \geq E_{th}$, introducing the maximum rate for inelastic collisions, $\nu_{\mathrm{in},0}$, if all molecules would get excited, analogous to Equation (9). Unlike ionization having a high E_{th}, this scenario is realistic for reactions with low E_{th} such as vibrational excitation. Based on Equations (10), (14) and (30), SEI can be expressed as

$$E_{\mathrm{pl}} = eE_p\frac{\nu_{e,\parallel}}{\nu_{\mathrm{in},0}} = \frac{\theta_{\mathrm{abs}}}{\nu_{\mathrm{in},0}} = m_e{\nu_{e,\parallel}}^2\frac{\nu_c}{\nu_{\mathrm{in},0}}. \tag{32}$$

Microscopically, E_{pl} largely depends on the kinetic energy of the electron drift motion in the plasma obtained by electron-neutral collisions provided to any inelastic collision.

The SEI can also be related to macroscopic (external) parameters, the absorbed power in the plasma, W_{abs}, and the molecular gas flow rate through the plasma, F_m, by

$$E_{\mathrm{pl}} = \frac{k_B T_0}{p_0} \frac{W_{\mathrm{abs}}}{F_m}, \tag{33}$$

(in [eV], which can be related to the energy density by 1 eV ≡ 4.3 J cm^{-3}) with temperature, T_0, and pressure p_0, at standard conditions (273.15 K, 101325 Pa).[38] Furthermore, the power taken from the electric field by the electrons (per unit volume, in [W m^{-3}]) for a plasma with a uniform electron density, n_e, can be related to the delivered power per plasma volume, V_{pl}, by[29]

$$P_{\mathrm{abs}} = n_e \theta_{\mathrm{abs}} = \frac{W_{\mathrm{abs}}}{V_{\mathrm{pl}}}. \tag{34}$$

Note that Equation (34) is a consequence of the electron energy balance in self-sustained low-temperature plasmas independent of the type of discharge,[27] which has been supported by experiments.[38,45] Regarding the residence time of the molecules in the plasma volume given by

$$\tau_{\mathrm{act}} = n_m \frac{V_{\mathrm{pl}}}{F_m} \frac{k_B T_0}{p_0}, \tag{35}$$

with the molecule density, n_m, SEI is eventually expressed as

$$E_{\mathrm{pl}} = \tau_{\mathrm{act}} \frac{n_e}{n_m} \theta_{\mathrm{abs}}, \tag{36}$$

thus combining microscopic and macroscopic parameters. With Equation (32) the relation

$$\tau_{\mathrm{act}} = \frac{n_m}{n_e \nu_{\mathrm{in},0}}, \tag{37}$$

is obtained (compared with Equation (23)), giving the residence time required for the full conversion of molecules by inelastic collisions in the plasma. Frequent collisions such as vibrational excitation or high electron densities require a shorter residence time than reactions with high energy thresholds.

Coming back to the definition of E_{pl} by Equation (33) and considering Equations (10) and (36), the SEI (in [eV]) is physically defined by

$$E_{\mathrm{pl}} = \frac{k_B T_0}{p_0} \frac{W_{\mathrm{abs}}}{F_m} = \frac{n_e}{n_m} \tau_{\mathrm{act}} \theta_{\mathrm{abs}} = \frac{n_e}{n_m} \tau_{\mathrm{act}} \nu_c \delta \bar{\varepsilon}. \tag{38}$$

Regarding Eq. (10) and $n_m = N$, it further follows that

$$E_{\mathrm{pl}} = \frac{n_e}{n_m} \tau_{\mathrm{act}} \theta_{\mathrm{abs}} = n_e \tau_{\mathrm{act}} \nu_{e,\parallel} \frac{eE_p}{N}. \tag{39}$$

Equations (38) and (39) thus relate the SEI to the mean electron impact energy and the reduced electric field, respectively. Note that in chemical kinetics models, E_{pl} is typically calculated by integrating the power deposition over the residence time, which agrees with Equation (39).[46] Contrary to the reduced electric field, E_p/N, which cannot easily be set by the operator, E_{pl} can be defined by macroscopic parameters, the (absorbed) power input per gas flow rate. While $\nu_{e,\parallel} \cdot E_p/N$ (see Equation (8)) can be quite different for DC and HF fields,[27,29] n_e can be adjusted by the power input (per plasma volume) and τ_{act} by the gas flow rate (per plasma volume). Unlike the EEDF, which describes the potential energy transfer in a single electron-neutral collision, E_{pl} comprises the energy transfer considering several inelastic collisions of (excited) molecules during their residence time, τ_{act}, in the plasma. Microscopically, the plasma properties are determined by the average power absorbed per electron independent of the used plasma source (see Equation (32)).

2.3 | Arrhenius-like behavior of a plasma-chemical activation mechanism

Since the energy available per molecule in the plasma is following a distribution law, not all molecules do react when the average value, E_{pl}, just meets the energy threshold, E_{th}, for the considered chemical reaction. If the energy distribution follows the Boltzmann distribution with $E_{\mathrm{pl}} = 3/2\ k_B T$ given as

$$f(E) = \frac{2}{\sqrt{\pi}} \left(\frac{3}{2E_{\mathrm{pl}}} \right)^{3/2} \sqrt{E}\ \exp\left(-\frac{3E}{2E_{\mathrm{pl}}} \right), \tag{40}$$

only the fraction of $exp(-1)$ of all molecules receives the required energy when $E_{\mathrm{pl}} = E_{\mathrm{th}}$, as shown in Figure 4a. For $E_{\mathrm{pl}} > E_{\mathrm{th}}$, the portion of collisions with sufficient energy is increasing following Arrhenius-like behavior, since the area under the graph from E_{th} to ∞ generates an $\exp(-E_{\mathrm{th}}/E_{\mathrm{pl}})$ form. Hence, Arrhenius-like activation reactions, where $k_B T$ is replaced by SEI, might determine many plasma-chemical activation mechanisms with an apparent activation barrier, E_{th}, for $E_{\mathrm{pl}} \geq E_{\mathrm{th}}$, as long as the considered activation mechanism prevails.

Considering a specific plasma-chemical reaction pathway with the energy barrier E_{th} in a molecular gas

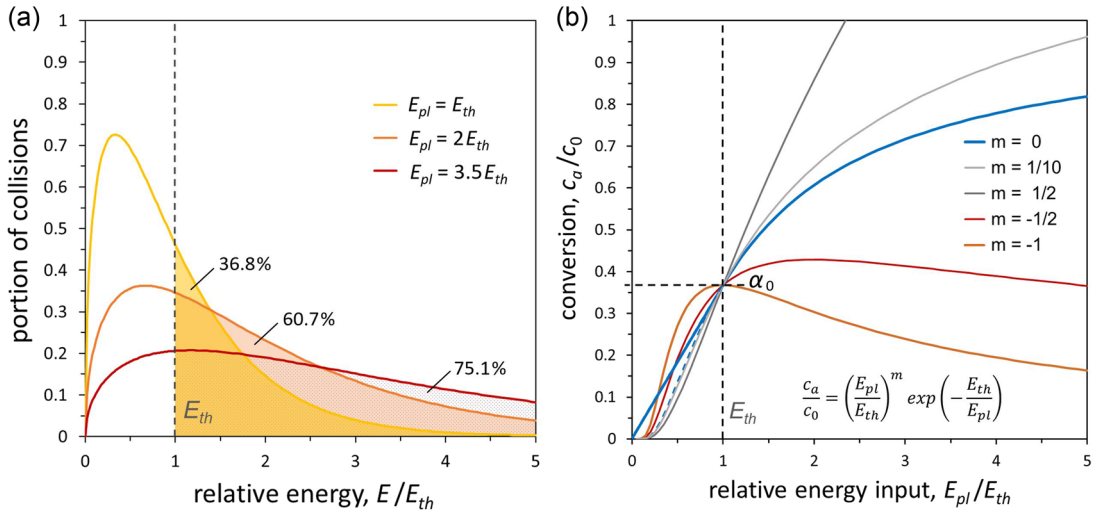

FIGURE 4 (a) Energy distribution according to Equation (40) for three different average energies E_{pl} with respect to E_{th}. The percentage gives the portion of collisions with energies above E_{th} following an Arrhenius-like form. (b) Characteristics of the modified Arrhenius equation with varying $(E_{pl}/E_{th})^m$ in the pre-exponential factor according to Equation (2). The curve for $m = -1$ (solid orange line) represents the reaction rate according to Equation (44). The solid blue line represents Equation (47), showing the difference of the linear regime for $E_{pl} < E_{th}$ to the Arrhenius curve (dashed blue line). All curves meet in one point, α_0 (normalized to c_0), denoted as "alpha point."

passing through the plasma zone, where the fraction a' of the inelastic collisions is contributing to the considered activation reactions, the energy lost per collision per second can be noted as

$$\theta_{l,a} = a'\theta_{abs} = a'\nu_{in,0}\, E_{pl} = \nu_{act,0}\, E_{pl}, \tag{41}$$

which is analogous to Equation (17).[38,40] For the lumped reaction rate, $\bar{\nu}_a$ (in $[s^{-1}]$), of the specific plasma-chemical reaction, it follows based on Equation (31) that

$$\bar{\nu}_a = \nu_{act,0} \exp\left(-\frac{E_{th}}{E_{pl}}\right) = \frac{a'\theta_{abs}}{E_{pl}} \exp\left(-\frac{E_{th}}{E_{pl}}\right). \tag{42}$$

This equation holds for $E_{pl} \geq E_{th}$, thus yielding a reaction rate depending on SEI and the fraction of power absorbed per electron lost into the activation reactions.[38] Again, $\nu_{act,0}$ can be seen as the ideal rate for plasma activation if either E_{th} would be zero, or if E_{pl} would exceed E_{th} in a way that all molecules react. Equation (42) is a modified Arrhenius equation similar to Equation (2) with $m = -1$ as displayed in Figure 4b.

For $E_{pl} \leq E_{th}$, it has been argued that the energy required for all excitation/dissociation reactions with energies below E_{th} can be assumed to be just of the order of E_{th} with the fraction a' contributing to the considered specific activation reaction[38,40]

$$\theta_{l,a} = a'\theta_{abs} \approx a' \sum_i \nu_i E_i = \nu_{act,0}\, E_{th}. \tag{43}$$

Excited states activated by electron impact at $E_i < E_{th}$ act as intermediates supporting the overall reaction with the threshold energy, E_{th}.

It thus follows for $E_{pl} \leq E_{th}$ considering Equations (41), (42) and (43) that

$$\begin{aligned} \bar{\nu}_a &= \nu_{act,0} \exp\left(-\frac{E_{th}}{a'\,\theta_{abs}/\nu_{act,0}}\right) \\ &= \frac{a'\theta_{abs}}{E_{th}} \exp(-1) = \alpha_0 a' \frac{\theta_{abs}}{E_{th}}. \end{aligned} \tag{44}$$

Hence, the maximum lumped rate for a low-temperature plasma activation mechanism, comprising all potential inelastic collisions contributing to the overall activation mechanism, following Arrhenius-like behavior, is fixed to $\alpha_0 = exp\,(-1)$, that is, ~36.8%, of the absorbed power of electrons provided for activation reactions, normalized to the related energy threshold. This finding is a consequence of the many excitation levels and intermediate states in a molecular plasma contributing to the chemical reaction pathway. Hence, $\bar{\nu}_a$ is approximately constant for $E_{pl} \leq E_{th}$, while it decreases for $E_{pl} \geq E_{th}$.

Considering now a rate equation for the low-temperature plasma activation mechanism yielding species of density, n_a, it can be written that

$$\frac{dn_a}{dt} = n_e \bar{\nu}_a, \tag{45}$$

with the lumped reaction rate, $\bar{\nu}_a$, at which the specific plasma-chemical reaction takes place in a closed system, that is, in the active plasma zone.[38,47] This rate equation for activation reactions can be further developed considering that activation occurs during the residence time of the molecules in the active plasma zone, τ_{act}, yielding the plasma-chemical conversion of the reactant into the activated product

$$c_a = \frac{\tau_{act}}{n_m}\frac{dn_a}{dt} = \tau_{act}\frac{n_e}{n_m}\bar{\nu}_a. \tag{46}$$

The factor $\tau_{act} \bullet n_e/n_m$ is a well-known reaction parameter that can be related to E_{pl} according to Equation (36).[38,48] Using Equations (42) and (44), the plasma-chemical conversion depending on E_{pl} can eventually be expressed by a linear and an Arrhenius-like regime as

$$c_a = E_{pl}\frac{\bar{\nu}_a}{\theta_{abs}} = c_0 \begin{cases} \alpha_0 \dfrac{E_{pl}}{E_{th}}, & E_{pl} \le E_{th} \\ \exp\left(-\dfrac{E_{th}}{E_{pl}}\right), & E_{pl} \ge E_{th} \end{cases}. \tag{47}$$

Different operational conditions (plasma source, reactor geometry, pressure) might affect the maximum conversion as given by

$$c_0 = \frac{\alpha}{\alpha_0} = a', \tag{48}$$

with $\alpha_0 = exp(-1)$, that is, α is the conversion at $E_{pl} = E_{th}$ and a' equals the maximum conversion, c_0. Figure 4b exemplarily shows the curve characteristics of some (modified) Arrhenius equations, including the linear regime for $E_{pl} \le E_{th}$ (for $m = 0$).

Following Equation (26), if a reaction pathway comprises several branches with similar E_{th}, averaging yields

$$\frac{c_a}{c_0} = \sum_i p_i \exp\left(-\frac{E_{th,i}}{E_{pl}}\right) = \exp\left(-\frac{\overline{E_{th}}}{E_{pl}}\right), \tag{49}$$

with $_{pi}$ the fraction for every branch i, yielding one apparent threshold energy, $\overline{E_{th}} = E_{th}$, which is thus the average over the considered reaction pathway.[44] On the contrary, if for example $E_{th,2}$ is sufficiently larger as $E_{th,1}$, the reaction pathway with $E_{th,1}$ prevails at lower E_{pl} (around $E_{th,1}$), while the second pathway becomes dominant at higher E_{pl} (exceeding $E_{th,2}$). Importantly, a gas molecule might undergo several inelastic collisions (or none) while traveling through the active plasma zone governed by the average available energy per molecule following a distribution law. Note that dissociation reactions yield $N > n_m$ during the residence time of one molecule in the plasma, while reactive species readily stick to surfaces, thus reducing N. These opposite effects might well be neglected in a flow system as commonly used in plasma processing.

3 | APPLICABILITY OF THE ARRHENIUS-LIKE APPROACH

Plasma polymerization and plasma gas conversion might be two fields that are predestined to apply the Arrhenius-like approach based on the SEI, since they comprise a plasma-chemical reaction pathway based on the many possibilities for inelastic collisions in molecular gases. The energy available in the plasma per molecule defines the possible plasma activation with a threshold energy yielding conversion of the starting molecules into a desired product.[1] While for plasma gas conversion gaseous products are seeked, reactive film-forming species are produced by plasma activation yielding a solid deposit, the plasma polymer, at surfaces surrounding the plasma. Examples for both fields are discussed in the following.

3.1 | Plasma polymerization

It has long been realized that dissociation of molecules in a plasma—such as, for example, methane—are governed by the SEI.[2] Soo Young Park et al. related the yield of plasma polymer deposition, that is, the conversion of monomer in the gas phase to the plasma polymer deposit in the solid phase, to a plasma-chemical activation step.[5,6] It was postulated that the activation step is a kind of "activated process" by the specific energy supplied per molecule that activates molecular bonds. Hence, an Arrhenius-like behavior with an apparent activation energy was inferred.

To relate SEI to plasma-chemical processes, a consistent and sufficiently precise measurement of the absorbed power in the plasma zone and the monomer gas flow rate through the plasma zone is required. W_{abs} might readily vary between 10% and 90% of the nominally applied power by the generator using different types of reactors and plasma sources. Furthermore, the

plasma expansion needs to be taken into account, that is, geometrical factors.[8] Well-defined conditions, for example, are given in a symmetric RF capacitively coupled plasma (CCP) set-up, enabling a rather constant plasma volume filling the full chamber between the plane parallel electrodes with distance, d, independent of power input and pressure. Due to the self-adjusting plasma zones with plasma length, d_{act} (active plasma zone), which depends on pressure, E_{pl} can be given by[38]

$$E_{pl} = \frac{k_B T_0}{p_0} \frac{W_{abs}}{F_m} \frac{d_{act}}{d}. \quad (50)$$

Likewise, E_{pl} can be assessed in asymmetric CCP or inductively coupled plasmas (ICPs) taking the plasma expansion into account given that the gas flow passes the active plasma zone.[8,49,50]

The plasma–chemical reaction pathway generates reactive film-forming species by activation reactions with the used monomer gas depending on SEI (i.e., E_{pl}). These species travel to the electrodes, chamber walls, and samples placed in the plasma chamber. A deposit forms at the surfaces regarding the sticking probability, s, of the incident species, that is, the likelihood that they are embedded in the growing film (and not leaving the chamber by the pumping system). Hence, a suitable way to assess conversion in plasma polymerization processes is the measurement of deposition rates. The mass deposition rate, R_m, normalized by monomer flow rate, F_m, and deposition area, A_{dep}, is then related to the fraction of activated molecules, c_a, that is, the conversion of monomer into film-forming species, by

$$R_m \frac{A_{dep}}{F_m} = s \frac{M_{dep}}{N_A} \frac{p_0}{k_B T_0} c_a, \quad (51)$$

with the mass of the deposited species, M_{dep}, and Avogadro's number, N_A.[38] Further normalizing by dividing Equation (51) by the mass of the used monomer molecule, M_{mol}, gives the dimensionless effective conversion yielding a deposit

$$c_{dep} = R_m \frac{A_{dep}}{F_m} \frac{N_A}{M_{mol}} \frac{k_B T_0}{p_0} = s \frac{M_{dep}}{M_{mol}} c_a, \quad (52)$$

which is thus smaller than the actual conversion in the gas phase. When the film-forming species and their sticking probabilities are known, the conversion in the gas phase can thus be derived depending on the SEI. Note that this approach is similar to Yasuda's seminal work by normalizing the deposited mass by the molecular mass of the considered monomers, which allows, for example, comparing plasma polymerization of homologous series of monomers.[51,52] Unlike using the SEI proportional to W_{abs}/F_m, which indicates the available energy for bond dissociation, Yasuda also normalized the reaction parameter using $W_{abs}/(F_m \bullet M_{mol})$— the so-called Yasuda parameter.[4] It should be noted that special care has to be taken to assess the "global" conversion in the gas phase considering that the deposition rates might vary on the electrode and the chamber walls.

Hexamethyldisiloxane (HMDSO, $(CH_3)_3$–Si–O–-Si–$(CH_3)_3$; $M_{mol} = 162\ g\ mol^{-1}$) is a well-studied monomer for plasma polymerization that shows a sticking probability of $s \approx 1$ due to the generation of highly reactive biradicals, $^{\bullet}$O–Si$^{\bullet}$–$(CH_3)_2$, as film-forming species ($M_{dep}/M_{mol} \approx 0.46$) using suitable plasma deposition conditions.[38] Polydimethylsiloxane (PDMS)-like films can thus be deposited. HMDSO might be used as a model molecule to apply the Arrhenius-like approach using different plasma operational conditions.[6,53–55] Optimum conversion of HMDSO into film-forming species can be achieved, for example, in an asymmetric CCP RF plasma at sufficiently high T_e and/or Ar admixture (Figure 5). Beside electron impact activation, Ar metastables (≥11.5 eV) also contribute to the transfer of energy to the molecules, that is, to the polymerizable gases.[56,57] Furthermore, the plasma-chemical reaction pathway of HMDSO activation involves a multistep mechanism via activated intermediates, including vibrational excitation followed by the removal of a $-CH_3$ group and opening of

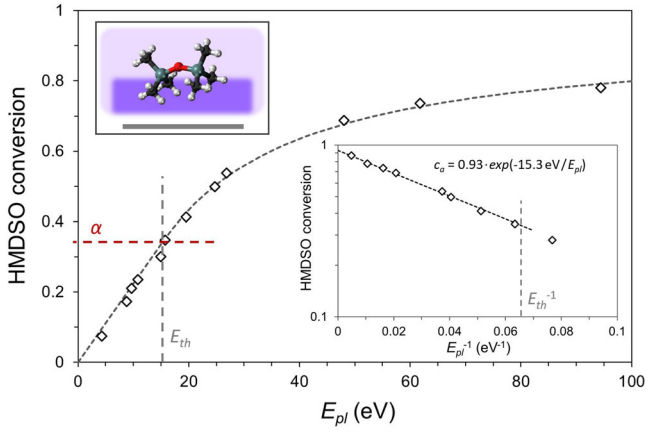

FIGURE 5 Conversion of hexamethyldisiloxane (HMDSO) into a deposit within an asymmetric capacitively coupled plasma (CCP) radio frequency (RF) plasma (Ar/HMDSO 1:1, 30 Pa; $T_e \approx 2$ eV). The assessment of the deposition rate at the RF-driven electrode (10 ×15 cm^2) indicates that the asymmetric set-up strongly promotes local deposition (93% at the electrode assuming optimum conversion). The inset diagram displays the related Arrhenius-like plot for $E_{pl} \geq E_{th}$, where $E_{th} \approx 15$ eV can be derived from the slope of the fit.

a Si–O bond. The activation energy for the overall reaction might thus slightly vary for the different possible pathways. On average, a threshold energy of 14–15 eV has been observed using different plasma geometries and plasma sources.[38]

Up to E_{th}, a linear increase in conversion can be noticed, while Arrhenius-like behavior is observed for higher energy input following Equation (47). The linear increase for $E_{pl} \leq E_{th}$ indicates that the assumption in Equation (43) might well be fulfilled, that is, the summated energy of all excitation/dissociation reactions is just of the order of E_{th} contributing to the plasma-chemical reaction pathway. Since for $E_{pl} > E_{th}$, on average, more energy per HMDSO molecule is available as required to form the biradical, $^{\bullet}O–Si^{\bullet}–(CH_3)_2$, further $–CH_3$ abstraction is promoted. Hence, M_{mol} is reduced on average, which can be considered to calculate c_a regarding the chemical film composition ranging from $SiOC_2$ (PDMS-like) to $SiO_{1.1}C_{1.7}$.[38] Following the Arrhenius-like approach, plasma polymer deposition can thus be optimized regarding conversion, that is, optimum use of resources, and also film properties. The highest functionality in terms of $–CH_3$ group retention within a cross-linked Si–O–Si backbone resulting in stable, hydrophobic PDMS-like PPFs is just obtained for E_{pl} around E_{th}. Aging effects have been observed for lower energy input, whereas increased energy input allows higher conversion albeit with an increasing number of trapped radical sites yielding post-plasma oxidation.[38,53] Furthermore, the plasma deposition process can be transferred to industrial size reactors maintaining optimum conversion, while simplified modeling defining the plasma zone as the origin of the known film-forming species allows optimizing distribution and homogeneity of film growth for large-area deposition. The hydrophobization of textiles and the corrosion protection of biomedical implants are just two examples.[58–60] Similarly, atmospheric plasma jets with HMDSO introduced in the postdischarge are used to locally deposit corrosion-resistant coatings on automotive parts.[61]

Besides organosilicon compounds, hydrocarbons are frequently used for plasma polymerization. Most of all, acetylene (C_2H_2) and ethylene (C_2H_4) as unsaturated monomers as well as ethane (C_2H_6) and methane (CH_4) as saturated hydrocarbon molecules are of interest for fundamental understanding. Those monomers were thus investigated based on the Arrhenius-like approach, both in low and atmospheric-pressure plasmas.[47,62,63] Here, a refined comparison is presented using a symmetric RF CCP plasma reactor with the same range of parameters (16 sccm of pure hydrocarbon gas at 7.5 Pa) for all monomers examined, enabling high conversion (yet not necessarily optimum conversion). Due to the symmetry of the reactor, the same uniform deposition rate was obtained on both electrodes of the same size, supporting the assessment of the global conversion. All four hydrocarbons show comparable threshold energy (slightly below 10 eV) for hydrocarbon abstraction by electron impact dissociative excitation.[64,65] Therefore, the experimental data of the normalized deposition rates yielding c_{dep} according to Equation (52) can be fitted with the Arrhenius-like approach at an energy input close to 10 eV and higher (Figure 6). Apparent threshold energies of 9–11 eV were attained with a linear increase in c_{dep} for lower energies. However, only the C_2H_2 plasma follows the Arrhenius fit over a broad range of $E_{pl} \geq E_{th}$, whereas the other three hydrocarbons tend to show a stronger increase in c_{dep} for higher energies.

Recall that c_{dep} still depends on sticking probability, s, which might change upon further hydrogen abstraction at increasing E_{pl}. In C_2H_2 plasma, mainly $^{\bullet}C_2H$ radicals are formed having a reported high sticking probability of 0.8 up to 0.92.[66,67] Assuming a value of $s \approx 0.9$ and that the plasma-chemical reaction pathway prevails over the entire range of examined energies, the conversion, c_a, of C_2H_2 into $^{\bullet}C_2H$ radicals can be derived. Using $c_{dep,max} = 0.55$ from the Arrhenius-like fit, it is found that $\alpha \approx 0.23$ (conversion at $E_{pl} = E_{th}$), that is, about 63% of the optimum conversion. Furthermore, assuming that a similar conversion is obtained for the other three hydrocarbons, their sticking probabilities around $E_{pl} \approx$

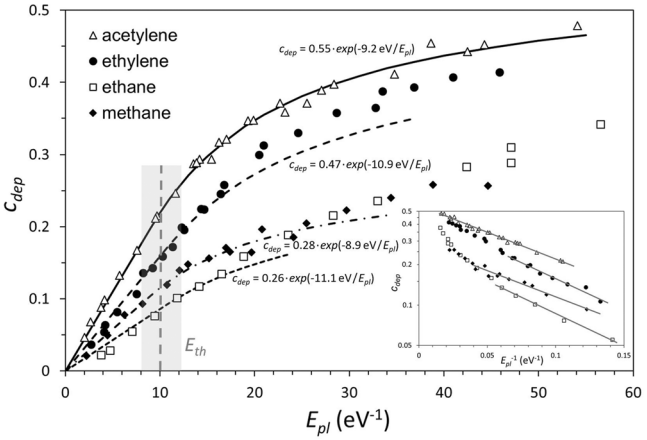

FIGURE 6 Sticking probability-dependent conversion of hydrocarbons into a deposit within a symmetric capacitively coupled plasma (CCP) radio frequency (RF) plasma (Ø 30 cm; 16 sccm, 7.5 Pa; $T_e \approx 2$ eV). The inset diagram displays the related Arrhenius-like plots for E_{pl} close to E_{th}, indicating the deflection from the fit at increasing E_{pl} (except for C_2H_2), likely due to the generation of film-forming species with higher sticking probabilities.

E_{th} can be inferred from the Arrhenius-like fit regarding M_{dep}/M_{mol} (Table 2).

The assessment of deposition rates depending on SEI gives further hints about the involved reaction mechanism for plasma activation. The derived E_{th} (of about 11 eV) and s (of about 0.8) for the C_2H_4 plasma, which are both higher as for $^{\bullet}C_2H_3$ radicals, indicate an additional reaction pathway yielding $^{\bullet}C_2H$ radicals by a multistep mechanism. With increasing E_{pl}, C_2H_4 conversion thus approaches C_2H_2 conversion, likely due to the prevailing contribution of $^{\bullet}C_2H$ radicals with higher s. Likewise, the plasma activation mechanisms of C_2H_6 and CH_4 can be understood by multistep reactions via activated intermediates. The conversion in a C_2H_6 plasma also approaches the one of C_2H_2 for increasing E_{pl}, which is known as "lost memory effect," that is, the plasma-activated products become independent of the used hydrocarbon compound.[68] For CH_4, $s \approx 0.65$ is obtained agreeing well with cavity experiments.[69] Note that the considered approach only covers gas phase reactions, while plasma-surface reactions might further abstract hydrogen from the growing film.[68] At elevated pressure, recombination reactions in the gas phase become important, and CH_4 plasmas also abundantly form C_2H_2.[69] Molecular dynamics simulations have also pointed out the important role of $^{\bullet}C_2H$ radicals in methane plasmas.[70]

From the above assessment, mainly C_2H_2 and C_2H_4 are well-suited polymerizable monomers used, for example, to deposit hard coatings or diffusion-controlling layers.[71–73] However, they do not bear interesting functionalities, which is why they are also mixed with nonpolymerizable gases such as N_2, NH_3, CO_2, CO, H_2O, O_2, and so on, to incorporate functional groups in a cross-linked hydrocarbon matrix. Importantly, the threshold energy for the hydrocarbon molecules, as derived from the Arrhenius-like approach, was found to be retained independent of the gas admixture.[74,75] Weak interaction of the polymerizable and nonpolymerizable gases in the plasma might thus be inferred for a broad parameter range, which agrees with observations made by Yasuda.[76] Since the plasma copolymerization with nonpolymerizable gases reduces the quantity of free radicals trapped in hydrocarbon plasma polymers, he assumed that the incorporation of the activated nonpolymerizable gases takes place during film growth by reacting with the free radicals. Remarkably, plasma reactions in CO_2/CH_4 mixtures at atmospheric pressure were also found to show parallel reaction pathways with negligible interactions in the gas phase.[77] The interaction at the surface can be used to enhance the stability of the plasma polymer films, which has led to hydrophilic plasma coatings that have been transferred to industrial processing.[78,79] While the presented approach thus enables insights into gas phase reactions, mainly for plasma state polymerization but also for gas conversion (as examined in the next section), further considerations are required involving surface reactions, which is out of the scope for this paper.

TABLE 2 Parameters for different molecules used in low-pressure plasma polymerization are derived from the Arrhenius-like approach.

Gas	E_{th} (eV) (observed)	Film-forming species ($E_{pl} \approx E_{th}$)	E_{th} (eV) (reported)	$\frac{M_{dep}}{M_{mol}}$	s (reported)	s ($E_{pl} \approx E_{th}$)
HMDSO	14–15	$^{\bullet}O–Si^{\bullet}–(CH_3)_2$	*multistep*	0.46		~1
C_2H_2	~9	$^{\bullet}C_2H$	7.5[a]	0.96	0.8[c]/0.92[d]	0.9[e]
C_2H_4	~11	$^{\bullet}C_2H_3$	6.75[a]	0.96	0.25[c]	
		$C_2H_2^* \rightarrow {}^{\bullet}C_2H$	*multistep*	0.89	~0.9	~0.8
C_2H_6	~11	$^{\bullet}C_2H_5$	7.45[a]	0.97	0.03[c]	
		$C_2H_4^* \rightarrow {}^{\bullet}C_2H_3/{}^{\bullet}C_2H$	*multistep*	0.9/0.83	0.25/~0.9	~0.55
CH_4	~9	$^{\bullet}CH_3/{}^{\bullet}CH_2$	8.8/8.6[b]	~0.9	<0.025[c]	
		$^{\bullet}CH_3^*/{}^{\bullet}CH_2^* \rightarrow {}^{\bullet}CH$	*multistep*	0.81		~0.65
		$\rightarrow {}^{\bullet}C_2H$	*recombination*			

Abbreviation: HMDSO, hexamethyldisiloxane.

[a]Electron impact dissociation data taken from Janev & Reiter.[64]

[b]Electron impact dissociation data taken from Reiter & Janev[65]

[c]Sticking probabilities taken from Bauer et al.[66]

[d]Sticking probability taken from Hopf et al.[67]

[e]Assumed sticking probability for $^{\bullet}C_2H$.

Finally, acrylic acid ($H_2C=CH–COOH$) plasmas might be mentioned as an example of a complex starting molecule that shows two distinct Arrhenius-like regimes.[13] At moderate E_{pl}, a threshold energy of about 7 eV can be observed indicating plasma activation of acrylic acid, while a second threshold energy at around 23 eV activates dissociative excitation strongly resembling CO_2/C_2H_4 gas mixtures. In this case, again, the stability of the functional plasma polymer films was found to be strongly enhanced.

3.2 | Plasma gas conversion

Plasma-driven CO_2 conversion into CO might be an interesting example to be studied in light of the SEI and to be connected to the Arrhenius-like approach.[80] The chemical reaction $CO_2 \rightarrow CO + ½\ O_2$ is obtained at the enthalpy of CO_2 dissociation, ΔH, of 2.9 eV. The energy transfer in the plasma comprises direct electron dissociation or dissociation through the so-called vibrational "ladder climbing."[81] Direct electron impact dissociation in a plasma occurs at a threshold energy of about 7 eV with a further contribution at about 10.5 eV, that is, noticeably higher than the dissociation energy to break one C–O bond in CO_2 of 5.5 eV.[82] To enable CO_2 conversion into CO at reduced energies, a plasma-chemical reaction pathway involving many vibrationally excited states, CO_2*, with small energy gaps and collisions among them, that is, vibrational ladder climbing, can be exploited allowing dissociation at 5.5 eV. Moreover, conditions that favor the further reaction of the generated side product, atomic oxygen, with CO_2 yield another CO molecule converted at 0.3 eV resulting in the overall specific energy requirement (threshold energy) of about 2.9 eV.[83] This reaction pathway thus requires a high collisional plasma (pressure higher than ~100 mbar) at limited SEI, that is, adjusted residence time, however, recombination and back reactions should be avoided.[84–86]

Low-pressure plasma conditions using RF excitation, on the contrary, generally do not support gas phase reactions among heavy species, thus promoting electron impact dissociation, also involving vibrationally excited intermediates. Only a few studies have thus been conducted using low pressure (and low temperature) RF plasmas for CO_2 conversion. For example, Zhang et al. used an ICP with varying power input (30–300 W) and CO_2 gas flow rate (10–100 sccm) diluted in Ar (1000 sccm) at a pressure of 14 Pa.[87] Ar admixture was found to increase the CO_2 conversion efficiency into CO, probably by enhancing the energy transfer to the molecules. Applying Equation (33), a broad range of SEI, that is, E_{pl}, from about 4.2–210 eV was covered, however, neglecting possible power losses dissipating in the copper coil during RF excitation. At the measured T_e of 2.0–2.5 eV, almost full conversion of CO_2 into CO was achieved at high SEI (Figure 7). The Arrhenius-like fit delivers an apparent activation energy of ~10 eV, which agrees well with the threshold energy, E_{th}, for direct electron impact dissociation of 7–8 eV by assuming power losses of 20%–30%.

Since the energy efficiency is defined as

$$\eta = c_a \frac{\Delta H}{E_{pl}}, \tag{53}$$

with $\Delta H = 2.9$ eV for CO_2 conversion, the attainable efficiency can be calculated depending on E_{pl}/E_{th}. Based on the Arrhenius-like behavior regarding Equations (47) and (48) it follows that

$$\eta = c_a \frac{\Delta H}{E_{pl}} = c_0 \frac{\Delta H}{E_{pl}} \exp\left(-\frac{E_{th}}{E_{pl}}\right). \tag{54}$$

The maximum efficiency is thus obtained for $E_{pl} = E_{th}$, reaching about 14% due to the required higher E_{th} compared with ΔH. For $E_{pl} < E_{th}$, the measured conversion as reported by Zhang et al. might follow a linear increase or might indicate enhanced conversion, which, however, remains unclear due to scarce data.[87]

Spencer and Gallimore also investigated RF-excited (13.56 MHz) low-pressure plasma conversion of CO_2 at high T_e of 2–4 eV and a pressure of 10–36 Pa (increasing

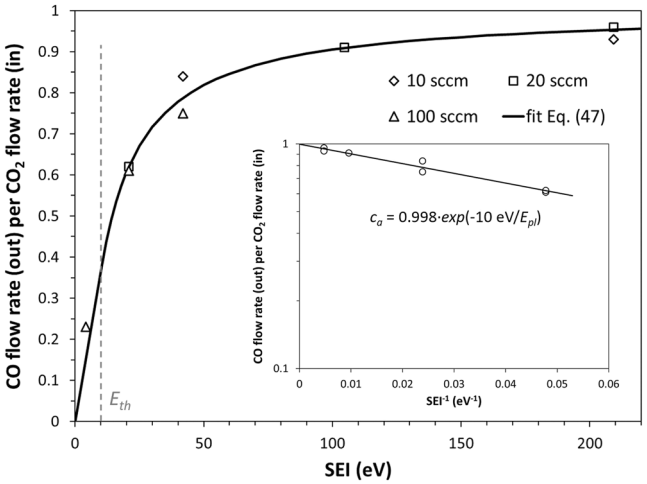

FIGURE 7 CO_2 conversion in an inductively coupled plasma (ICP) radio frequency (RF) plasma at low pressure depending on specific energy input (SEI) approaching full conversion at high energies. The apparent threshold energy is derived neglecting possible power losses. Data taken from Zhang et al.[87]

with CO_2 flow rate) that favors electron impact dissociation.[88] While clearly the same trend of conversion versus SEI was observed, the use of different pressures for every experimental series and low power coupling (as reflected by their reported high SEI based on nominal power per CO_2 flow rate), however, resulted in noticeable spreading of the observed data. As conclusion, optimum conversion can be reached with low pressure and low-temperature RF plasmas at high T_e following Arrhenius-like behavior, however, at limited energy efficiency. Furthermore, by precisely measuring the SEI in a CO_2 plasma, the threshold energy for CO_2 dissociation by electronic excitation might be clarified, while experiments at low energies (below E_{th}) would help to understand whether enhanced conversion is supported in low-temperature plasmas.

To enhance conversion, MW plasmas at elevated pressure are studied, which also induce an enhanced gas temperature, T_{gas} (3000–6000 K).[89] Such conditions support effective excitation to vibrational states, which can lead to the so-called ladder climbing effect.[80] Hecimovic et al. reported a maximum CO_2 conversion of ~31% at the SEI of 2.9 eV using a plasma torch experiment at 2.45 GHz and 200 mbar.[90] The generated vortex configuration in the used quartz tube combined with MW excitation is thought to favor vibrational excitation, and a CO/O_2 ratio of around two was observed. As depicted in Figure 8, the conversion was found to be slightly enhanced for $E_{pl} < E_{th}$ up to the (expected) threshold energy of 2.9 eV compared with the linear/Arrhenius-like fitting of Equation (47) considering a maximum conversion of $c_0 \approx 0.95$. Due to the high T_{gas} the CO_2 conversion was considered predominantly driven by thermal dissociation. Importantly, the gas composition was sampled at two positions, in the hot gas and after passing a heat exchanger, thus reaching thermally equilibrated conditions. By sampling only the central hot part of the plasma, the authors could show that high local conversions might be measured resulting in high efficiencies for $E_{pl} < E_{th}$, even exceeding 100%.[90] Great care should thus be taken to assess values for the global conversion that need to be considered for the presented Arrhenius-like approach.

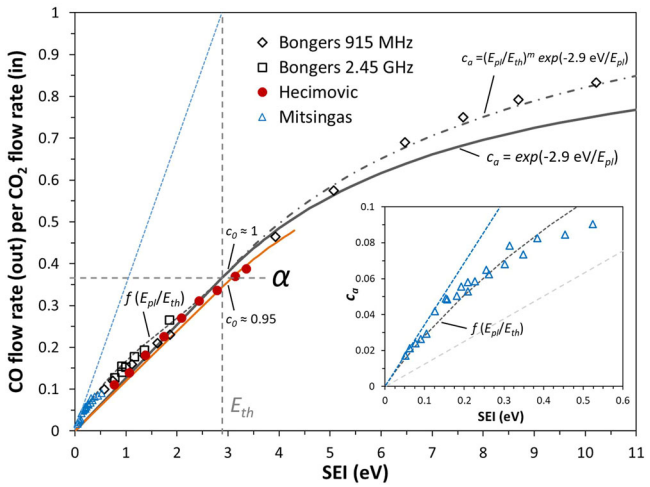

FIGURE 8 CO_2 conversion using MW plasma covering a broad range of SEI (E_{pl}). The conversion for $E_{pl} < E_{th}$ exceeds the linear fit according to Equation (47). Also at higher SEI (above E_{th}) an enhanced conversion is observed as compared to the Arrhenius-like behavior. Data taken from Bongers et al., Hecimovic et al., and Mitsingas et al., where the inset shows an enlargement of the data at low SEI.[85,90,91]

Likewise, Bongers et al. examined CO_2 conversion in two different MW plasma set ups at 915 MHz and 2.45 GHZ, reaching maximum conversion conditions with enhanced conversion for $E_{pl} < E_{th}$.[85] Again, the high T_{gas} might support predominant thermal dissociation of CO_2. Interestingly, enhanced CO_2 conversion was also attained by increasing E_{pl} above E_{th} (Figure 8), due to the conversion of surplus energy to heat, which will be further discussed below. As another example, Mitsingas et al. investigated CO_2 conversion using a direct-coupled MW plasma system at atmospheric pressure with a rather low SEI (< 1 eV).[91] Remarkably, as shown in Figure 8, a nearly linear increase that would approach full conversion at $E_{pl} = E_{th}$ was observed for SEI < 0.1 eV. This means that there is indeed an effective mechanism which transfers the entire plasma energy to a few molecules that undergo the demanded chemical reaction, while all other molecules remain in their thermal energy state. This mechanism can thus be expected to be promoted at suitable (elevated) temperatures. Due to constraints by entropy, however, this is only possible for the limit of SEI approaching zero, since a distribution of energies is observed with increasing SEI. Therefore, the gradient of conversion increase is steadily reduced, while constantly revealing enhanced conversion compared with the linear part of Equation (47).

The many possibilities for excitation in CO_2 plasmas yield a high cross section for inelastic collisions for low electron impact energies (see also Figure 1).[92] Most of all, the asymmetric stretching mode of vibrational excitation for CO_2 followed by vibration–vibration relaxation collisions favors gradual population of the higher vibrational levels, finally leading to dissociation with $E_{th} = 2.9$ eV due to ladder climbing.[81,82] It can thus be assumed that the probability that a specific activation reaction takes place for $E_{pl} < E_{th}$ can be higher as given by Equation (43), since CO_2* intermediates also transfer energy among each other pushing some to higher levels.

Based on Equations (43) and (47), it generally follows that

$$c_a = E_{pl}\frac{\bar{\nu}_a}{\theta_{\text{abs}}} = \frac{\theta_{l,a}}{\theta_{\text{abs}}} f\left(\frac{E_{\text{pl}}}{E_{\text{th}}}\right) = c_0 f\left(\frac{E_{\text{pl}}}{E_{\text{th}}}\right). \quad (55)$$

As corroborated by the discussed experimental data using MW plasmas and expected constraints, the function $f\left(\frac{E_{\text{pl}}}{E_{\text{th}}}\right)$ takes the value of zero with a slope of 1 at $E_{\text{pl}}/E_{\text{th}} = 0$ and approaches $exp(-1)$ at $E_{\text{pl}} = E_{\text{th}}$ in a continuous way, that is, reaching the slope of $exp(-1)$, as shown in Figure 8. In Equation (47), on the contrary, the slope equals $exp(-1)$ for all $E_{\text{pl}} < E_{\text{th}}$ (linear regime) and follows Arrhenius-like behavior for $E_{\text{pl}} \geq E_{\text{th}}$, due to the distribution of energy—as typically observed for plasma activation in plasma polymerization processes.

These data can be further discussed regarding energy efficiency. Based on Equations (53) and (54), the energy efficiency for $E_{\text{pl}} \geq E_{\text{th}}$ can be expressed as a function of conversion, yielding

$$\eta = c_0 \frac{\eta}{c_{\text{a}}} \exp\left(-\frac{\eta}{c_{\text{a}}}\frac{E_{\text{th}}}{\Delta H}\right), \quad (56)$$

and finally

$$\eta = -\frac{\Delta H}{E_{\text{th}}} c_a \ln\left(\frac{c_{\text{a}}}{c_0}\right). \quad (57)$$

Figure 9 represents experimental data and fits based on Equation (57) for optimum conditions, that is, $c_0 = 1$. While the (optimum) efficiency, η, with $\Delta H = E_{\text{th}} = 2.9$ eV can easily be derived for $E_{\text{pl}} \geq E_{\text{th}}$, the limiting conditions for the function $f\left(\frac{E_{\text{pl}}}{E_{\text{th}}}\right)$ suggests to transform Equation (57) for $E_{\text{pl}} \leq E_{\text{th}}$ by mirroring, scaling, and moving (see Supporting Information) to obtain a function that is continuous at $E_{\text{pl}} = E_{\text{th}}$, that is, at $c_{\text{a}} = \alpha$ such as

$$\eta = \frac{\Delta H}{E_{\text{th}}}\left[c_0 + \frac{1-\alpha_0}{\alpha_0} c_{\text{a}} \ln\left(\frac{c_{\text{a}}}{c_0}\right)\right], \quad (58)$$

with $\alpha_0 = \alpha/c_0 = exp(-1)$. Equation (58) is also plotted in Figure 9 for optimum conditions ($\Delta H = E_{\text{th}}$, $c_0 = 1$). Thus, a slide-shaped function results with the connecting point at $\eta = c_{\text{a}} = \alpha$, the alpha point, where the gradient is zero —as, to some extent, an equivalent to the Stoletow point for ionization.[32] Using this function and Equation (53), the conversion for $E_{\text{pl}} < E_{\text{th}}$ can be derived. From

$$c_{\text{a}}\frac{\Delta H}{E_{\text{pl}}} = \frac{\Delta H}{E_{\text{th}}}\left[c_0 + \frac{1-\alpha_0}{\alpha_0} c_{\text{a}} \ln\left(\frac{c_{\text{a}}}{c_0}\right)\right]. \quad (59)$$

it follows that

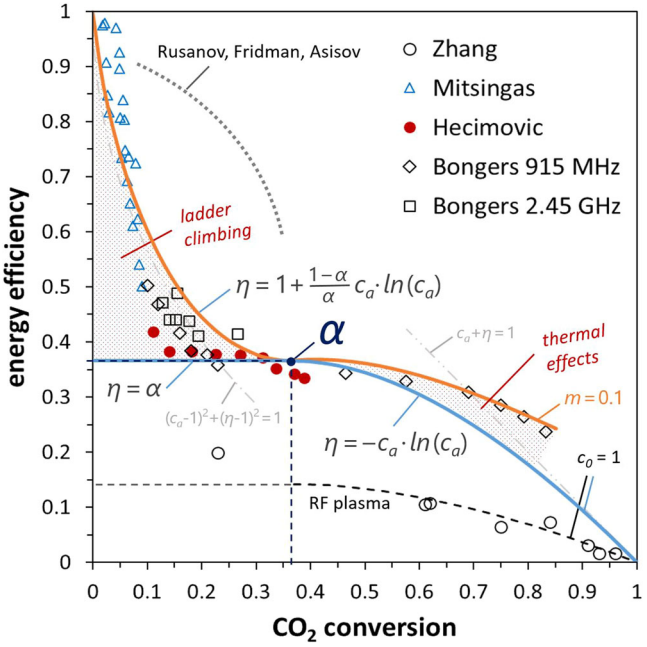

FIGURE 9 Energy efficiency, η, as a function of CO_2 conversion, c_{a}. The experimental data were used as in Figures 7 and 8. Note that the measurement error might be rather high toward low conversion. The bold blue curve with $\eta = \alpha$ for $E_{\text{pl}} \leq E_{\text{th}}$ represents the optimum according to the Arrhenius-like approach for low-temperature plasmas. Enhanced efficiencies, as given by the bold orange slide-shaped curve might thus indicate additional energy transfer, also considering the range for $E_{\text{pl}} \geq E_{\text{th}}$ by the factor $(E_{\text{pl}}/E_{\text{th}})^m$, here with $m = 0.1$. Limiting cases for low and high c_{a}/η are drawn by dash-dotted gray lines. The fit for low-temperature RF plasma (dashed black curve) reflects the higher E_{th} of 7-8 eV. The dotted dark gray curve indicates the best efficiencies as reported by Rusanov et al.[81,83,93]

$$\frac{E_{\text{pl}}}{E_{\text{th}}} = \frac{\frac{c_{\text{a}}}{c_0}}{1 + \frac{1-\alpha_0}{\alpha_0}\frac{c_{\text{a}}}{c_0}\ln\left(\frac{c_{\text{a}}}{c_0}\right)}. \quad (60)$$

This function that is equivalent to Equation (55) cannot be analytically solved for c_{a}/c_0 but easily plotted (as has been used for Figure 8 with $c_0 = 1$), yielding an appropriate fit regarding the spreading of the data at low E_{pl}. Compared with the Arrhenius-like form (see Equation (47) for $E_{\text{pl}} \leq E_{\text{th}}$) using $\Delta H = E_{\text{th}}$

$$\frac{E_{\text{pl}}}{E_{\text{th}}} = \frac{c_a}{\eta} = \frac{c_a}{\alpha_0 c_0}, \quad (61)$$

as obtained for electron impact-activated low-temperature plasmas, the denominator in Equation (60) just gives the enhancement factor involving ladder climbing (see Supporting Information).

In this way, the function displayed by the bold blue line in Figure 9 describes the optimum energy efficiency

that can be achieved for a demanded gas conversion by electron impact plasma activation in low-temperature plasmas, where E_{pl} covers all inelastic collisions following a distribution law. A directed energy transfer among (vibrationally) excited species, such as ladder climbing, might enhance the conversion at a given E_{pl} below E_{th}, resulting in higher efficiencies as compared with the linear regime of the Arrhenius-like approach. Note that further enhanced conversion resulting in even higher energy efficiencies were reported for $E_{pl} < E_{th}$ by Rusanov et al. dating back to the 1980ies.[81,83,93] Those experimental data that have yet to be reproduced by others are comprehensively summarized and discussed, for example, by Bogaerts et al.[80,94] and will not be further analyzed here. It might be recalled, however, that special care has to be taken by assessing global CO_2 conversion as discussed above.

As mentioned before, Bongers et al. also observed enhanced conversion for $E_{pl} > E_{th}$. Under all conditions examined, the gas temperature, T_{gas}, was found to be in excess of 4000 K, which is why predominant thermal dissociation was assumed.[85] Thermal effects typically increase with SEI, for example, by increasing the residence time in the high-temperature region of the plasma. Hence, a T-dependence of the pre-exponential factor might be considered yielding a modified Arrhenius equation as in Equation (2), with E_{pl} still replacing k_BT in the exponential term. Assuming that the increase in T_{gas} (or in the size of the high-temperature region) is roughly proportional to E_{pl}, the factor $(E_{pl}/E_{th})^m$ can be introduced in the pre-exponential factor of the conversion equation (Equation (55) or Eq. (47)), yielding for $E_{pl} \geq E_{th}$

$$c_a = c_0 \left(\frac{E_{pl}}{E_{th}}\right)^m \exp\left(-\frac{E_{th}}{E_{pl}}\right). \quad (62)$$

A satisfactory fit using this approximation can be found for $m \approx 0.1$, at least up to a few times E_{pl}/E_{th} before c_a approaches c_0 (see Figures 4 and 8), probably constrained by the thermal equilibrium limit (see Supporting Information).[80] The enhanced conversion efficiency for CO_2 at $E_{pl} > E_{th}$, fitted in Figure 9 by using Equations (53) and (62) with $\Delta H = E_{th}$ and $c_0 = 1$, might thus be analyzed involving thermal effects. Plasma activation as the base reaction yields numerous excited states with increasing SEI that can be more efficiently converted thanks to additional thermal energy.[95,96] In this way, T_{gas} increases the number of collisions between the excited molecules during the residence time in the plasma, which can be reflected by the modified pre-exponential factor. In a similar way, using an MW plasma torch as a heat source for plasma methane pyrolysis ($T_{gas} \approx 4000$ K), an almost linear increase in CH_4 conversion with SEI up to a conversion above E_{th} exceeding 60% (probably revealing a small dip below $c_a \approx 0.4$) has been recently reported, agreeing with curves as shown in Figure 4 for positive m.[97] Such T_{gas}-related effects might be further investigated compared with plasma activation for low-temperature plasmas as described by the Arrhenius-like approach.

Remarkably, a distinctive point is observed at $E_{pl} = E_{th}$ yielding $\eta = c_a = \alpha$ for all conditions, denoted as alpha point, giving a maximum value of $\alpha_0 = exp(-1) \approx 0.368$ for $c_0 = 1$. Recent work by Mercer et al. using a vortex-stabilized MW reactor with a 2.45 GHz magnetron also showed that the optimization of CO_2 conversion and efficiency approaches the maximum of $exp(-1)$.[98] The occurrence of this distinctive point indicates that additional energy transfer enhancing the conversion of the chemical reaction might proceed differently for $E_{pl} < E_{th}$ and $E_{pl} > E_{th}$ as described by the slide-shaped curve centered at the alpha point. For low SEI, the available energy can effectively be distributed into vibrational excitation of CO_2 resulting in ladder climbing up to E_{th}, which might be supported by T_{gas} causing particles to have more energy. Moreover, electron kinetics were found to be affected by T_{gas}.[99] Hence, the probability that colliding particles have sufficient energy for plasma activation (by electrons and among excited particles) can exceed $\alpha_0 \bullet E_{pl}/E_{th}$, yielding an enhanced efficiency (>36.8%). However, the number of CO_2 molecules to reach the threshold for dissociation remains low, thus limiting conversion (<36.8%). For SEI above E_{th}, gas heating allows to transfer more energy over τ_{act} for a given E_{pl}, for example, due to an enlarged high-temperature region, considering E_{pl} as defined in Equation (36). Conversion and efficiency might thus be enhanced by $(E_{pl}/E_{th})^m$. A high CO_2 conversion (~75%) with reasonable efficiency (~30% compared with ~20% for low-temperature plasmas) has been reached, for example, for $E_{pl} \approx 3.5 \bullet E_{th}$ (an optimization that is also often used for plasma polymerization).[85] A thorough analysis of CO_2 conversion based on the introduced Arrhenius-like approach considering electron impact-initiated inelastic collisions for low-temperature plasmas might help to clarify the different aspects of energy transfer in plasma activation processes, also extending experiments at low temperature such as in low-pressure RF plasmas.

4 | SUMMARY

The SEI has been microscopically and macroscopically derived showing that it is based on the energy uptake by electrons in the plasma distributed to inelastic collisions

(see Equations (32), (33), (36), and (39)), which is driven by the externally applied power input per gas flow rate delivered to the active plasma zone:

$$\begin{aligned} \mathrm{SEI} = E_{\mathrm{pl}} &= \frac{\theta_{\mathrm{abs}}}{\nu_{\mathrm{in},0}} = n_e \tau_{\mathrm{act}} \frac{\theta_{\mathrm{abs}}}{n_m} = n_e \tau_{\mathrm{act}} \nu_{e,\parallel} \frac{eE_p}{N} \\ &= \frac{k_B T_0}{p_0} \frac{W_{\mathrm{abs}}}{F_{\mathrm{m}}}. \end{aligned} \tag{63}$$

The SEI thus defines the average energy available per molecule in the plasma for plasma activation and plasma-chemical reactions with respect to the corresponding threshold energy, E_{th}.

Following the classical Townsend mechanism for ionization, the probability for a direct electron impact ionizing collision to occur shows Arrhenius-like behavior, where the (reduced) electric field strength or the electron impact energy replaces k_BT. Likewise, plasma activation of molecules via inelastic collisions can be described by an Arrhenius-like behavior, where it is more convenient to use SEI as the energy parameter to replace k_BT. As distinguished from ionization as in noble gases, low-temperature plasmas with molecular gases involve intermediate states with activation energies below E_{th} to support a demanded plasma-chemical reaction having the activation barrier E_{th}. Therefore, the considered reaction can occur more frequently for $E_{\mathrm{pl}} < E_{\mathrm{th}}$, however, still with limited conversion due to the energy distribution in plasmas. Based on electron impact inelastic collisions involving intermediates (see Equation (43)), the conversion increases at maximum with $E_{\mathrm{pl}}/E_{\mathrm{th}}$ up to E_{th} resulting in

$$\frac{c_a}{c_0} = \begin{cases} \alpha_0 \dfrac{E_{\mathrm{pl}}}{E_{\mathrm{th}}}, & E_{\mathrm{pl}} \le E_{\mathrm{th}} \\ \exp\left(-\dfrac{E_{\mathrm{th}}}{E_{\mathrm{pl}}}\right), & E_{\mathrm{pl}} \ge E_{\mathrm{th}} \end{cases}, \tag{64}$$

(which is equivalent to Equation (47)) and is limited to $\alpha_0 = exp(-1)$ at $E_{\mathrm{pl}} = E_{\mathrm{th}}$. Hence, also the energy efficiency is limited to α_0 ("alpha point") for low-temperature plasmas. This behavior has been observed for many different monomers as used for plasma polymerization and might also be the basis to describe low-temperature plasma gas conversion.

For plasma gas conversion, however, additional energy transfer into the demanded chemical reaction is observed in different ways for $E_{\mathrm{pl}} < E_{\mathrm{th}}$ and $E_{\mathrm{pl}} > E_{\mathrm{th}}$. At low SEI, thermally enhanced ladder climbing via vibrationally excited states with small energy gaps support dissociation at the minimum energy required to promote the chemical reaction at E_{th}, while the surplus energy above E_{th} enables an increasing size of the high-temperature region yielding an increasing number of collisions during the residence time in the plasma. Based on experimental data from the literature, a conversion enhancement factor, CEF, as compared with the linear/Arrhenius-like form of Equation (64) for low-temperature plasmas, is suggested:

$$\mathrm{CEF} = \begin{cases} \alpha_0{}^{-1}\left(1 + \dfrac{1-\alpha_0}{\alpha_0}\dfrac{c_a}{c_0}\ln\left(\dfrac{c_a}{c_0}\right)\right), & E_{\mathrm{pl}} \le E_{\mathrm{th}} \\ \left(\dfrac{E_{\mathrm{pl}}}{E_{\mathrm{th}}}\right)^m, & E_{\mathrm{pl}} \ge E_{\mathrm{th}} \end{cases}. \tag{65}$$

Note that the alpha point is conserved by this provisional analysis (see Supporting Information). This approach might thus provide a different point of view to discuss energy transfer yielding plasma activation based on SEI, which needs to be further elaborated.

5 | CONCLUSIONS AND PERSPECTIVES

Introducing the SEI (SEI or E_{pl}) in plasmas comprising molecular gases, the energy transfer by the electric field to the molecules via inelastic collisions can be governed by one parameter that is microscopically (Equation 32) and macroscopically (Equation 33) defined. Unlike the EEDF describing the potential energy transfer in a single electron-neutral collision, E_{pl} comprises the energy transfer considering several inelastic collisions in the plasma during the electron confinement time as well as inelastic collisions with excited molecules during their residence time. For a specific plasma-chemical reaction pathway, only a fraction of the inelastic collisions might contribute to the related plasma activation mechanism. Using an approach based on the probability for plasma activation to occur, that is, to convert the starting molecule into a desired product, Arrhenius-like behavior can be expected for $E_{\mathrm{pl}} \geq E_{th}$, that is, for energy above the apparent threshold energy for plasma activation, similar to the classical Townsend mechanism for ionization. While for direct electron impact reactions, no activation would occur for electron impact energies below E_{th}, as, for example, excitation in noble gases, the many excitation states in molecular gases enable intermediates that promote the plasma activation mechanism also for $E_{\mathrm{pl}} < E_{th}$ beside the distribution of energies.

Considering plasma polymerization to deposit a desired plasma polymer film, typically a linear increase in conversion into film-forming species in the gas phase,

which can directly be related to deposition rates, is observed for SEI up to E_{th}, followed by Arrhenius-like behavior, as long as one dominant reaction pathway prevails. With a change in gas composition due to increased dissociation, different plasma-chemical pathways might occur depending on the range of SEI. The presented (simplified) approach can thus be used to investigate plasma polymerization processes based on the average energy available per molecule, independent of pressure, to gain insights into the plasma polymerization mechanism, to optimize conversion and film properties, and to scale plasma processes. Furthermore, deviations of the Arrhenius-like behavior might not only indicate different reaction pathways but can also point to a nonlinear dependence of power absorption on external parameters. The reactor set-up might thus be improved. The low-temperature plasma provides special (nonequilibrium) conditions to physically activate plasma-chemical reaction pathways in the gas phase. Electron impact creates reactive intermediates governed by SEI yielding film growth of irregular "plasma polymer" structures. Further energy delivered during plasma-surface interaction contributes additionally to the irregularity of plasma polymer films, which has not been discussed here. The plasma environment, however, still comprises chemical features even at high SEI, favoring, for example, sticking of C_2H species using hydrocarbon monomers.

Likewise, plasma gas conversion is based on plasma activation mechanisms and can be examined in a similar way. For example, global CO_2 conversion was assessed regarding optimum conversion and energy efficiency. Enhanced conversion compared with a linear increase for $E_{pl} \leq E_{th}$ indicate an efficient (directed) activation mechanism via collisions among intermediates, which is known as vibrational ladder climbing. Thus, the type and rate of inelastic collisions determine the reaction pathway at low SEI. The analytical description of the low and high energy range with respect to the threshold energy for CO_2 conversion based on the Arrhenius-like approach yields a unique, slide-shaped curve for the efficiency as a function of conversion. This curve matches well with experimental results from the last few years. Importantly, a distinctive point can be derived, the so-called alpha point, where both efficiency and conversion can reach a maximum of 36.8%. It might be mentioned that the underlying function $-x \cdot ln\ x$ is also known as "entropy term" having a maximum entropy at $x = 0.368$.[100] One might thus speculate whether a connection with the alpha point exists. To further elucidate additional ways of energy transfer affecting the energy distribution as described by the Arrhenius-like approach, further investigations are required, involving also low-temperature plasma gas conversion conditions (avoiding thermal effects) as reference.

Generally, energy efficiencies are key for plasma-based chemical production such as CO_2 conversion to become a competitive technology.[80,101] Some limitations of gas conversion using plasma technology might thus be taken into account according to the performed analysis based on the Arrhenius-like approach, probably among other constraints.[102] However, high conversion might become more important than efficiency—as it is already the case with the field of plasma polymerization. The increasing use of renewable energy results in "free" peak energy that needs to be valued in a useful way. Here, plasma gas conversion that can be at all times electrically switched on and off without requiring heating cycles is an attractive method to yield valuable products that can be stored and transported.

As a final remark, the fields of plasma polymerization and plasma gas conversion might benefit from each other, since they both consider plasma activation and plasma-chemical reaction pathways.

ACKNOWLEDGMENTS

Dirk Hegemann would like to acknowledge valuable discussions with Annemie Bogaerts, University of Antwerp, Belgium and Ramses Snoeckx, KAUST, Saudi Arabia about CO_2 conversion in plasmas. Open access funding provided by ETH-Bereich Forschungsanstalten.

DATA AVAILABILITY STATEMENT

The data that supports the findings of this study are largely available from the literature. Further data are available from the corresponding author upon reasonable request.

ORCID

Dirk Hegemann http://orcid.org/0000-0003-4226-9326

REFERENCES

[1] H. Drost, *Plasmachemie*, Akademie-Verlag, Berlin, Germany **1978**.
[2] H.-E. Wagner *in:* Low Temperature Plasma Physics (ed. Hippler et al.), Wiley-VCH, Weinheim, Germany **2001**, pp. 305ff.
[3] D. D. Neiswender, *Adv. Chem. Ser.* **1969**, *80*, 338.
[4] H. Yasuda, T. Hirotsu, *J. Polym. Sci. Polym. Chem. Ed.* **1978**, *16*, 743.
[5] S. Y. PARK, N. Kim, U. Y. Kim, S. I. Hong, H. Sasabe, *Polym. J.* **1990**, *22*, 242.
[6] S. Y. Park, N. Kim, *J. Appl. Polym. Sci.* **1990**, *46*, 91.
[7] N. Spiliopoulos, D. Mataras, D. E. Rapakoulias, *Appl. Phys. Lett.* **1997**, *71*, 605.
[8] D. Hegemann, M. M. Hossain, E. Körner, D. J. Balazs, *Plasma Processes Polym.* **2007**, *4*, 229.
[9] F. Bally-Le Gall, A. Mokhter, S. Lakard, S. Wolak, P. Kunemann, P. Fioux, A. Airoudj, S. El Yakhlifi,

C. Magnenet, B. Lakard, V. Roucoules, *Plasma Processes Polym*. **2019**, *16*, 1800134.
[10] N. H. Le, M. Bonne, A. Airoudj, P. Fioux, R. Boubon, D. Rebiscoul, F. Bally-Le Gall, B. Lebeau, V. Roucoules, *Plasma Processes Polym*. **2021**, *18*, 2000183.
[11] M. Michlíček, L. Blahová, E. Dvořáková, D. Nečas, L. Zajíčková, *Appl. Surf. Sci*. **2021**, *540*, 147979.
[12] C. Oehr, M. Müller, B. Elkin, D. Hegemann, U. Vohrer, *Surf. Coat. Technol*. **1999**, *116–119*, 25.
[13] D. Hegemann, E. Körner, S. Guimond, *Plasma Processes Polym*. **2009**, *6*, 246.
[14] P. Barboun, P. Mehta, F. A. Herrera, D. B. Go, W. F. Schneider, J. C. Hicks, *ACS Sustain. Chem. Eng*. **2019**, *7*, 8621.
[15] J. Kim, D. B. Go, J. C. Hicks, *Phys. Chem. Chem. Phys*. **2017**, *19*, 13010.
[16] N. Turan, M. Saeidi-Javash, Y. Zhang, D. B. Go, *Plasma Processes Polym*. **2022**, *19*, 2200011.
[17] Z. Sheng, Y. Watanabe, H. H. Kim, S. Yao, T. Nozaki, *Chem. Eng. J*. **2020**, *399*, 125751.
[18] S. Arrhenius, *Z. Phys. Chem*. **1889**, *4*, 226.
[19] S. R. Logan, *J. Chem. Educ*. **1982**, *59*, 279.
[20] K. J. Laidler, *Physical Chemistry*, 1st ed., Benjamin/Cummings, US **1982**, pp. 376.
[21] I. W. M. Smith, *Chem. Soc. Rev*. **2008**, *37*, 812.
[22] K. J. Laidler, *J. Chem. Educ*. **1984**, *61*, 494.
[23] K. Sharp, F. Matschinsky, *Entropy* **2015**, *17*, 1971.
[24] J. F. Friedrich, J. Meichsner, *Nonthermal Plasmas for Materials Processing*, John Wiley & Sons, Hoboken, NJ, USA **2022**, pp. 72ff.
[25] R. I. Golyatina, S. A. Maiorov, *Plasma Phys. Rep*. **2022**, *48*, 193.
[26] T. Shirai, T. Tabata, H. Tawara, *At. Data Nucl. Data Tables* **2001**, *79*, 143.
[27] V. A. Godyak, *IEEE Trans. Plasma Sci*. **2006**, *34*, 755.
[28] S. Pancheshnyi, S. Biagi, M. C. Bordage, G. J. M. Hagelaar, W. L. Morgan, A. V. Phelps, L. C. Pitchford, *Chem. Phys*. **2012**, *398*, 148.
[29] M. Moisan, J. Pelletier, *Physics of Collisional Plasmas*, Springer, Dordrecht, Netherlands **2012**, pp. 339ff.
[30] J. Townsend, *Electricity in Gases*, Oxford University Press, London, UK **1915**, pp. 290ff.
[31] A. von Engel, Electron-Emission Gas Discharges I **1956**, 504. ed. S. Flügge. Springer, Berlin, Germany.
[32] J. R. Roth, *Industrial Plasma Engineering, Volume I (Principles)*, Institute of Physics Publishing, Bristol, UK **1995**, pp. 240ff.
[33] T. Aoyama, *Nuclear Instruments and Methods in Physics Research Section A: Accelerators, Spectrometers, Detectors and Associated Equipment* **1985**, *234*, 125.
[34] G. Auriemma, D. Fidanza, G. Pirozzi, C. Satriano, *Nuclear Instruments and Methods in Physics Research Section A: Accelerators, Spectrometers, Detectors and Associated Equipment* **2003**, *513*, 484.
[35] A. von Engel, *Gas Discharge Physics*, Taylor & Francis, London, UK **1983**, pp. 76ff.
[36] B. M. Smirnov, *Theory of Gas Discharge Plasma*, Springer, Cham, Switzerland **2015**, pp. 199ff.
[37] G. Franz, *Low Pressure Plasmas and Microstructuring Technology*, Springer, Heidelberg, Germany **2009**, pp. 103ff.
[38] D. Hegemann, E. Bülbül, B. Hanselmann, U. Schütz, M. Amberg, S. Gaiser, *Plasma Processes Polym*. **2021**, *18*, 2000176.
[39] G. Janzen, *Plasmatechnik*, Hüthig, Heidelberg, Germany **1992**.
[40] K. Behringer, *Plasma Phys. Controlled Fusion* **1991**, *33*, 997.
[41] Y. Itikawa, *J. Phys. Chem. Ref. Data* **2006**, *35*, 31.
[42] Y. Chang, C. A. Ordonez, *Chem. Phys*. **1998**, *231*, 27.
[43] D. A. Diver, L. F. A. Teodoro, C. S. MacLachlan, H. E. Potts, *arXivarXiv preprint arXiv:0810.1763*. **2008**.
[44] N. E. Blanchard, B. Hanselmann, J. Drosten, M. Heuberger, D. Hegemann, *Plasma Processes Polym*. **2015**, *12*, 32.
[45] N. Hershkowitz, J. Ding, R. A. Breun, R. T. S. Chen, J. Meyer, A. K. Quick, *Phys. Plasmas* **1996**, *3*, 2197.
[46] S. Heijkers, R. Snoeckx, T. Kozák, T. Silva, T. Godfroid, N. Britun, R. Snyders, A. Bogaerts, *J. Phys. Chem. C* **2015**, *119*, 12815.
[47] D. Hegemann, *J. Phys. D Appl. Phys*. **2013**, *46*, 205204.
[48] A. Rutscher, H. E. Wagner, *Contrib. Plasma Phys*. **1985**, *25*, 337.
[49] D. Hegemann, E. Körner, S. Chen, J. Benedikt, A. von Keudell, *Appl. Phys. Lett*. **2012**, *100*, 051601.
[50] D. Hegemann, M. Michlíček, N. E. Blanchard, U. Schütz, D. Lohmann, M. Vandenbossche, L. Zajíčková, M. Drábik, *Plasma Processes Polym*. **2016**, *13*, 279.
[51] C. P. Ho, H. Yasuda, *J. Appl. Polym. Sci*. **1990**, *39*, 1541.
[52] H. Yasuda, *Luminous Chemical Vapor Deposition and Interface Engineering*, Marcel Dekker, New York, NY **2005**.
[53] D. Hegemann, H. Brunner, C. Oehr, *Plasmas Polymers* **2001**, *6*, 221.
[54] D. Hegemann, B. Nisol, S. Watson, M. R. Wertheimer, *Plasma Chem. Plasma Process*. **2017**, *37*, 257.
[55] D. A. Zuza, V. O. Nekhoroshev, A. V. Batrakov, A. B. Markov, I. A. Kurzina, *Vacuum* **2023**, *207*, 111690.
[56] O. Krogh, T. Wicker, B. Chapman, *J. Vac. Sci. Technol. A* **1986**, *4*, 1796.
[57] D. Loffhagen, M. M. Becker, D. Hegemann, B. Nisol, S. Watson, M. R. Wertheimer, C. P. Klages, *Plasma Processes Polym*. **2020**, *17*, 1900169.
[58] D. Hegemann, *Ind. J. Fibre Text. Res*. **2006**, *31*, 99.
[59] C. Oehr, D. Hegemann, M. Liehr, P. Wohlfart, *Plasma Processes Polym*. **2022**, *19*, 2200022.
[60] Y. Wang, Y. Li, Z. Li, L. Ren, *ACS Appl. Mater. Interfaces* **2022**, *14*, 56169.
[61] D. B. Salem, D. Pappas, M. Buske, *Plasma. Process. Polym*. **2023**, *20*, e2200211.
[62] D. Hegemann, B. Nisol, S. Watson, M. R. Wertheimer, *Plasma. Process. Polym*. **2016**, *13*, 834.
[63] D. Hegemann, B. Nisol, S. Gaiser, S. Watson, M. R. Wertheimer, *Phys. Chem. Chem. Phys*. **2019**, *21*, 8698.
[64] R. K. Janev, D. Reiter, *Phys. Plasmas* **2004**, *11*, 780.
[65] D. Reiter, R. K. Janev, *Contrib. Plasma Phys*. **2010**, *50*, 986.
[66] M. Bauer, T. Schwarz-Selinger, W. Jacob, A. von Keudell, *J. Appl. Phys*. **2005**, *98*, 073302.
[67] C. Hopf, T. Schwarz-Selinger, W. Jacob, A. von Keudell, *J. Appl. Phys*. **2000**, *87*, 2719.
[68] A. von Keudell, *Thin Solid Films* **2002**, *402*, 1.

[69] E. Delikonstantis, M. Scapinello, G. D. Stefanidis, *Fuel Process. Technol.* **2018**, *176*, 33.
[70] G. O. Kandjani, P. Brault, M. Mikikian, G. Tetard, A. Michau, K. Hassouni, *Plasma. Process. Polym.* **2023**, *20*, e2200192.
[71] M. Weiler, S. Sattel, T. Giessen, K. Jung, H. Ehrhardt, V. S. Veerasamy, J. Robertson, *Phys. Rev. B: Condens. Matter Mater. Phys.* **1996**, *53*, 1594.
[72] N. Boutroy, Y. Pernel, J. M. Rius, F. Auger, H. J. Bardeleben, J. L. Cantin, F. Abel, A. Zeinert, C. Casiraghi, A. C. Ferrari, J. Robertson, *Diamond Relat. Mater.* **2006**, *15*, 921.
[73] B. R. Coad, P. Favia, K. Vasilev, H. J. Griesser, *Plasma Processes Polym.* **2022**, *19*, 2200121.
[74] D. Hegemann, E. Körner, K. Albrecht, U. Schütz, S. Guimond, *Plasma Processes Polym.* **2010**, *7*, 889.
[75] D. Hegemann, U. Schütz, E. Körner, *Plasma Processes Polym.* **2011**, *8*, 689.
[76] H. Yasuda, *Plasma Polymerization*, Academic Press, Orlando, FL **1985**, pp. 115ff.
[77] P. Navascués, J. Cotrino, A. R. González-Elipe, A. Gómez-Ramírez, *SSRN* **2023**. https://doi.org/10.2139/ssrn.4270153
[78] M. M. Hossain, D. Hegemann in:Textile Dyeing ed. P. Hauser (Ch. 9), IntechOpen, London, UK **2011**, pp. 173.
[79] A. G. Guex, F. M. Kocher, G. Fortunato, E. Körner, D. Hegemann, T. P. Carrel, H. T. Tevaearai, M. N. Giraud, *Acta Biomater.* **2012**, *8*, 1481.
[80] R. Snoeckx, A. Bogaerts, *Chem. Soc. Rev.* **2017**, *46*, 5805.
[81] A. Fridman, *Plasma Chemistry*, Cambridge University Press, Cambridge, UK **2008**.
[82] A. Bogaerts, W. Wang, A. Berthelot, V. Guerra, *Plasma Sources Sci. Technol.* **2016**, *25*, 055016.
[83] V. D. Rusanov, A. A. Fridman, G. V. Sholin, *Soviet Phys. Uspekhi* **1981**, *24*, 447.
[84] T. Kozák, A. Bogaerts, *Plasma Sources Sci. Technol.* **2014**, *23*, 045004.
[85] W. Bongers, H. Bouwmeester, B. Wolf, F. Peeters, S. Welzel, D. van den Bekerom, N. den Harder, A. Goede, M. Graswinckel, P. W. Groen, J. Kopecki, M. Leins, G. van Rooij, A. Schulz, M. Walker, R. van de Sanden, *Plasma Processes Polym.* **2017**, *14*, 1600126.
[86] A. Hecimovic, F. A. D'Isa, E. Carbone, U. Fantz, *J. CO2 Utilization* **2022**, *57*, 101870.
[87] D. Zhang, Q. Huang, E. J. Devid, E. Schuler, N. R. Shiju, G. Rothenberg, G. van Rooij, R. Yang, K. Liu, A. W. Kleyn, *J. Phys. Chem. C* **2018**, *122*, 19338.
[88] L. F. Spencer, A. D. Gallimore, *Plasma Chem. Plasma Process.* **2011**, *31*, 79.
[89] G. Chen, R. Snyders, N. Britun, *J. CO2 Utilization* **2021**, *49*, 101557.
[90] A. Hecimovic, F. D'Isa, E. Carbone, A. Drenik, U. Fantz, *Rev. Sci. Instrum.* **2020**, *91*, 113501.
[91] C. M. Mitsingas, R. Rajasegar, S. Hammack, H. Do, T. Lee, *IEEE Trans. Plasma Sci.* **2016**, *44*, 651.
[92] K. H. Kim, K. Y. Kim, Y. H. Hong, H. J. Moon, C. W. Chung, *Phys. Plasmas* **2019**, *26*, 123516.
[93] R. I. Asisov, A. K. Vakar, V. K. Jivotov, M. F. Krotov, O. A. Zinoviev, B. V. Potapkin, A. A. Rusanov, V. D. Rusanov, A. A. Fridman, *Proc. USSR Acad. Sci.* **1983**, *271*, 94.
[94] A. Bogaerts, E. C. Neyts, *ACS Energy Lett.* **2018**, *3*, 1013.
[95] K. H. R. Rouwenhorst, H. G. B. Burbach, D. W. Vogel, J. Núñez Paulí, B. Geerdink, L. Lefferts, *Catal. Sci. Technol.* **2021**, *11*, 2834.
[96] Z. Sheng, S. Kameshima, K. Sakata, T. Nozaki *in:*Plasma Chemistry and Gas Conversion ed. N. Britun, T. Silva (Ch. 3), IntechOpen, **2018**, pp. 1.
[97] S. Kreuznacht, M. Purcel, S. Böddeker, P. Awakowicz, W. Xia, M. Muhler, M. Böke, A. Keudell, *Plasma Processes Polym.* **2023**, *20*, 2200132.
[98] E. R. Mercer, S. Van Alphen, C. F. A. M. van Deursen, T. W. H. Righart, W. A. Bongers, R. Snyders, A. Bogaerts, M. C. M. van de Sanden, F. J. J. Peeters, *Fuel* **2023**, *334*, 126734.
[99] A. W. van de Steeg, L. Vialetto, A. F. S. Silva, P. Viegas, P. Diomede, M. C. M. van de Sanden, G. J. van Rooij, *J. Phys. Chem. Lett.* **2022**, *13*, 1203.
[100] A. Wehrl, *Rev. Mod. Phys.* **1978**, *50*, 221.
[101] D. S. Mallapragada, Y. Dvorkin, M. Modestino, D. V. Esposito, W. Smith, B. M. Hodge, M. P. Harold, V. M. Donnelly, A. Nuz, C. Bloomquist, K. Baker, L. C. Grabow, Y. Yan, N. N. Rajput, R. Hartman, E. J. Biddinger, E. Aydil, A. Taylor, *ChemRxiv* **2022**. https://doi.org/10.26434/chemrxiv-2022-00gls
[102] E. Thimsen, *AIChE J.* **2021**, *67*, e17291.

SUPPORTING INFORMATION

Additional supporting information can be found online in the Supporting Information section at the end of this article.

How to cite this article: D. Hegemann, *Plasma Processes Polym.* **2023**;20:e2300010. https://doi.org/10.1002/ppap.202300010